Enhanced Understanding of Network Losses: WP3-5 Report

Ilias Sarantakos
David Greenwood
Peter Davison
Charalampos Patsios

Contents

1. Introduction

1.1. Project Context

Enhanced Understanding of Network Losses is a project which seeks to enable DNOs to better understand, and make decisions pertaining to, the unavoidable losses which take place in their networks. The project is broken down into five work packages. This report describes the activities completed in, and learning arising from, WPs 3-5.

In a previous report, WP1 reviewed the state of the art in loss estimation and loss reduction in both academic literature and industrial practice, discussing methods for resolving the variability of demand; estimating the impact of low-carbon technologies, including harmonic currents; the impact of load imbalance; methods for estimating the impedance of Low Voltage networks; and assessing the impact of measurement error and data granularity on the accuracy of loss estimation. The key findings have been summarised in four categories i.e. the impact of present and future network scenarios including the variability of demand and generation, the impact of Smart and non-Smart Technology, the impact of measurement errors, and the impact of measuring at multiple aggregation levels. In a subsequent report and paper, we revealed the effects of demand growth on losses and their estimation in traditional networks.

In WP2, we investigated the value of data in understanding and quantifying losses; thus focusing on three of the four categories identified above. This was carried out in two stages: first gathering and analysing network data from multiple sources, including SCADA, project data, representative profiles, and forecasted data; and secondly performing sensitivity analyses using a first iteration of our modelling framework, in order to capture:

- the value of data, including the amount, sampling rate, quality, and accuracy
- the effects of network topology considering both urban and rural configurations
- the effects of measurement location and the level of data aggregation

In this final report – which describes the work carried out in, and learning arising from, WPs 3, 4, and 5 – we present a method developed to enable estimation of losses in real networks based on a subset of generic networks. We then investigate losses in a DSO environment by considering how losses will be affected by a more active distribution network. Finally, we introduce a hypothesis that losses can be used by the DSO as an

adaptive market signal to influence the behaviour of active network users and deliver better utilised and more reliable distribution networks.

1.2. Losses in a DSO Environment

Network losses are an unavoidable reality of transporting electricity from generators to end-users via transmission and distribution networks. In previous reports we have discussed how losses are not straightforward to calculate because of their non-linear relationship with electricity demand. We have also identified uncertainty in the way network measurements and models are used to estimate losses. In this report, we seek to inform answers around two overarching questions regarding the role of losses in active distribution networks managed by a DSO as a neutral market facilitator:

1. What value does a DSO gain from an enhanced understanding of network losses, and can this be used to influence the behaviour of active network users?
2. Based on findings around Question 1, to what extent should network losses, and the resulting cost to end users, be included in DSO decision making?

As we identified in WP 1, in the current GB regulatory environment DSOs are not directly accountable for network losses as they are in many other countries. Network losses are a function of both the physical makeup of the network and the way in which the network is used. The DSO is responsible for the former but have little control over the latter. Simplistically speaking, network losses are equal to I^2R, where R is determined by the network and I (which as a squared term will be more influential) is determined by the network users. This suggests that network users have a greater influence on network losses than the DSO.

Network losses give a strong indication of how heavily utilised a network is; if real-time losses are included in network tariffs then this can provide a self-correcting incentive to move network use to periods with lower use, and therefore lower losses. Consequently, our hypothesis is this: While network losses are not a significant concern for a DSO, they can be a powerful tool to influence the behaviour of active network users and thereby deliver more affordable, sustainable, and reliable networks for all customers.

1.3. Distinctiveness of Approach and Key Findings

The adopted approach can help progress the understanding around network losses considering existing academic literature and industrial practices in the following ways:

1. We introduce a distinctive method for estimating network losses based on representative feeders. These are produced through a clustering process that considers nine distinctive feeder characteristics that can influence losses. The method offers flexibility in terms of: a) the properties of the feeders selected as inputs to the clustering algorithm and b) the dependency of the representative feeder to the one for which the losses are estimated, based on criteria such as the load distribution factor. In this way losses can be estimated with a high degree of confidence for any given set of feeders and loading conditions. This can prove a useful tool as both the network configuration and loading patterns are likely to change as more flexibility and new operations are introduced in distribution networks.
2. Our findings suggest that the introduction of improved loss calculation and estimation methods such as the one discussed in the previous point, in conjunction with the use of more frequent and accurate network measurements, can result in significantly overall improved network operation. We will show that when a DNO specifically targets loss reduction through active decision-making, customer benefits, such as network reliability are minimally affected, while network efficiency is significantly improved. At the same time, secondary benefits, such as an improvement in voltage profile have also been observed.
3. In a similar fashion, we will show that when network participants (e.g. those dispatching distributed energy resources) are encouraged to incorporate losses into their decision-making this can result in increased network capacity for these types of flexibility. We have observed a direct relationship between the strength of this incentive, signalled by the DNO and the risk of network constraint violations.

Up to now, and for HV and below, generic methods have been used to calculate losses such as generic LLFs as discussed in the Literature Review section. These rely on formulas using approximations, estimations of consumption based on quarterly data from customer bills, and sporadic measurements. Even in the networks which feature bespoke loss analysis, this is conducted after-the-fact, while our findings suggest there is significant value in the DSO having visibility of losses in real time. Based on the analysis and results in this report, such traditional approaches could significantly impede the ability of DSOs to capture the aforementioned benefits.

1.4. Report Structure

Section 2 describes a loss estimation method based on feeder clustering and transforming loss calculations for representative feeders to give loss estimates for real feeders. Sections 3 and 4 describe studies using methods for reducing network losses which are fully controlled by the DSO (network reconfiguration and soft open points), whilst considering other benefits these could provide to the system. Section 5 shows how active network users – in this case a high penetration of aggregated electric vehicles – can affect network losses, and how the DSO can take actions using losses as a market signal to reduce costs for consumers and improve the hosting capacity of the network. Section 5 discusses the implications of the findings, and section 6 provides conclusions for the report and the project.

2. Feeder Clustering and Estimation of Losses

2.1. Introduction and Process Overview

Electrical losses in distribution networks (DNs) are estimated rather than calculated for several reasons, including the absence of metering, the size and number of these networks [1], and the availability and accuracy of measured data. This section presents a method to group similar feeders according to several predefined characteristics. This results in a specific number of groups (which are called clusters), each of which is represented by a representative feeder. Power losses can then be calculated for each representative feeder; subsequently losses can be estimated for any feeder based on the loss of the associated representative feeder. Figure 1 gives an overview of the clustering process employed in this section.

In [1], the length and resistance of main feeder and laterals, the number of laterals, as well as the number of customers were employed as clustering variables (or characteristics). Indeed, these characteristics significantly affect network losses. To improve this method, we replaced number of customers with peak demand, and we also included load factor and load distribution factor (LDF). Peak demand along with the load factor represents much more accurately the level of loading on the feeder than the number of customers. LDF provides information about the distance of the load points from the substation and is explained further below.

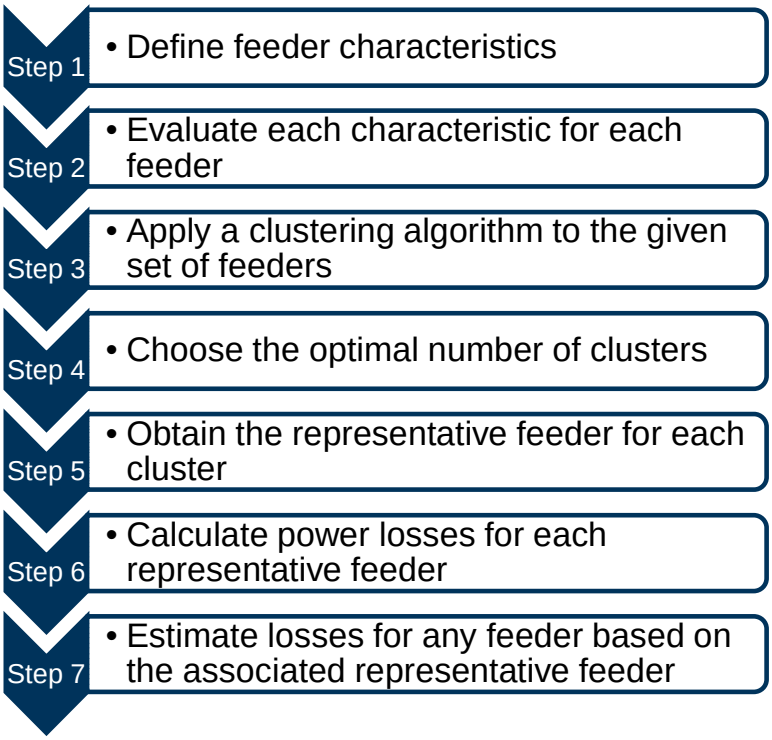

Figure 1: Overview of the clustering process.

2.2. Network and Data

Haxby Road primary DN (see Figure 2) has been used for this study, which is an 11 kV urban network with seven feeders and 56 load points corresponding to 11,740 customers. Peak demand – based on Element Energy data [2] – of each feeder is presented in Figure 3.

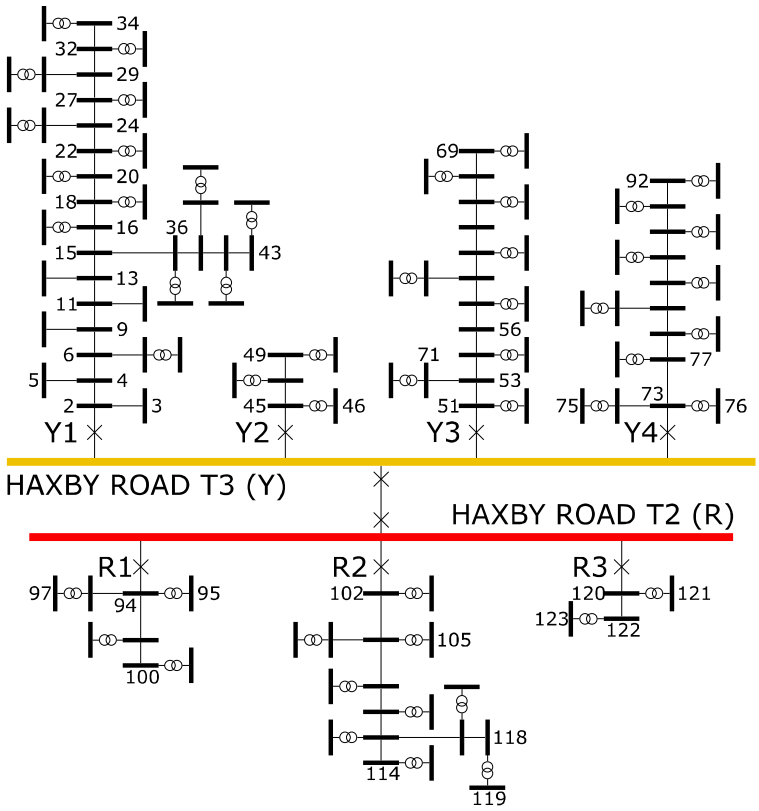

Figure 2: Haxby Road primary distribution network.

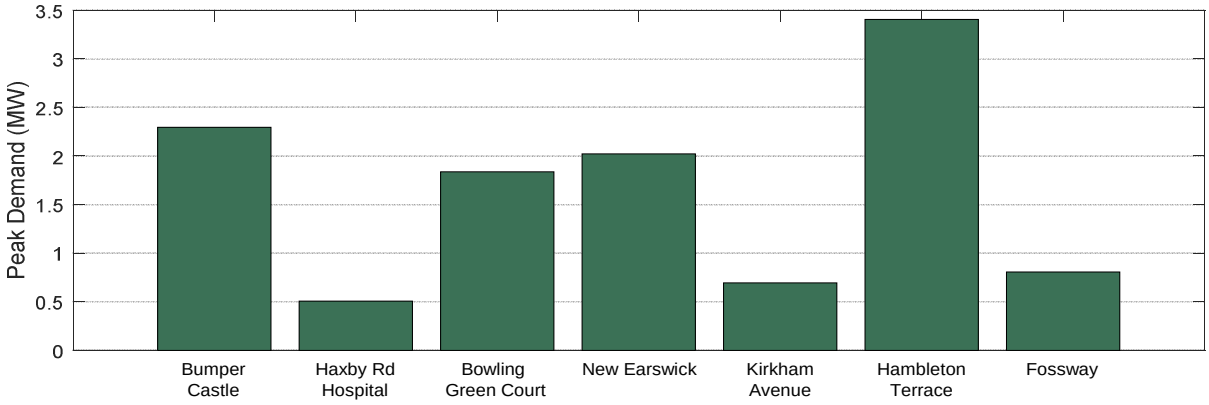

Figure 3: Peak demand of each feeder of the Haxby Road network.

2.3. Clustering Process

The input to the clustering algorithm was the seven feeders of Haxby Road DN and another 13 synthesized feeders based on the original ones. Expert judgment was employed to populate the characteristics of the synthesized feeders ensuring reasonable variation between their characteristics within a pragmatic range. Our analysis showed that for the cases explored raising the number of synthesized feeders further yielded no significant changes in the clustering output. Nine characteristics were chosen that influence the estimation of network losses. These characteristics are listed below:

1) Length of main feeder
2) Length of laterals
3) Number of laterals
4) Resistance of main feeder
5) Resistance of laterals
6) Peak demand
7) Number of load points
8) Load factor
9) Load distribution factor (LDF)

LDF is defined as

$$LDF = \frac{\sum_i P_i L_i}{P \cdot L} \tag{2.1}$$

where P_i is the power of load point i; L_i is the distance of load point i from the substation; P is the total demand of the feeder; and L is the length of the feeder. It expresses the distribution of load across the feeder, with zero corresponding to a case which the total demand of the feeder is located at the substation (i.e. $L_i = 0$ for each load point i); and one corresponding to a case where the total demand is located at the endpoint of the feeder (i.e. $L_i = L$ for all load points).

The 20 (7 real + 13 synthesized) feeders with the values for the nine aforementioned characteristics are presented in Table I.

Table I: The set of feeders to which the clustering algorithm will be applied.

Feeder Name-Number /Feature	Length of main feeder (km)	Length of laterals (km)	Number of laterals	Resistance of main feeder (pu)	Resistance of laterals (pu)	Peak Demand (MW)	Number of load points	Load Factor	Load Distribution Factor
Bump. Castle (1)	7.667	3.585	6	1.25	0.818	2.2958	19	0.4848	0.7744
Haxby R. H. (2)	1.402	0	0	0.18	0	0.508	3	0.5285	0.9082
Bowl. Gr. Ct (3)	8.01	0.72	2	1.2	0.136	1.8363	9	0.4861	0.7214
New Earswick (4)	6.057	1.262	2	1.146	0.38	2.022	10	0.516	0.6137
Kirkham Ave. (5)	1.992	0.359	1	0.244	0.049	0.6959	4	0.367	0.61
Hambl. Tce (6)	3.636	1.23	2	0.44	0.148	3.4062	9	0.3417	0.525
Fossway (7)	0.658	0	0	0.144	0	0.8057	2	0.3408	0.6464
Synth. Feeders									
(8)	1	0	0	0.16	0	0.45	3	0.32	0.65
(9)	2	0	0	0.35	0	1.75	5	0.45	0.55
(10)	1.5	0	0	0.28	0	0.75	4	0.34	0.62
(11)	0.7	0	0	0.1	0	0.7	2	0.53	0.7
(12)	2.5	0.4	1	0.375	0.08	0.9	5	0.47	0.71
(13)	5	0.7	2	0.8	0.15	1.5	8	0.5	0.65
(14)	7.5	1.2	3	0.975	0.252	2.4	12	0.54	0.68
(15)	8	1	3	1.36	0.19	1.98	11	0.37	0.72
(16)	9	1.4	4	1.44	0.21	2.55	17	0.39	0.74
(17)	6	0.85	2	0.96	0.255	2.1	10	0.48	0.69
(18)	4.5	0.72	2	0.585	0.1656	1.8	10	0.34	0.6
(19)	3.5	0.6	2	0.42	0.15	1.2	8	0.52	0.54
(20)	2	0.33	1	0.38	0.0627	1.8	6	0.48	0.63

We have applied two clustering algorithms (which have been widely used in the relevant literature, e.g. [3, 4]) on the set of feeders that was presented above. Firstly, *k*-means++ was applied. *k*-means++ is an iterative algorithm which partitions the observations (here feeders) of an $n \times m$ (here 20×9) data matrix into k clusters, and returns n cluster indices of each observation based on a specific distance metric. Euclidean distance metric is the most commonly used. The steps of the algorithm can be found in [5]. Clustering evaluation is then performed using the silhouette criterion [6]. The silhouette value for each point is a measure of how similar that point is to points in its own cluster, when compared to points in other clusters. The silhouette value S_i for the ith point is defined as:

$$S_i = \frac{b_i - a_i}{\max(a_i, b_i)} \tag{2.2}$$

where a_i is the average distance from the ith point to the other points in the same cluster as i, and b_i is the minimum average distance from the ith point to points in a different cluster, which is calculated for all clusters.

The silhouette value ranges from –1 to 1. A high silhouette value indicates that i is well matched to its own cluster, and poorly matched to other clusters. If most points have a high silhouette value (quantified using the mean silhouette value below), then the clustering solution is appropriate. If many points have a low or negative silhouette value, then the clustering solution might have too many or too few clusters. We have used the mean silhouette value to select the optimal number of clusters as illustrated in Figure 4; we obtain the best match when number of clusters = 3.

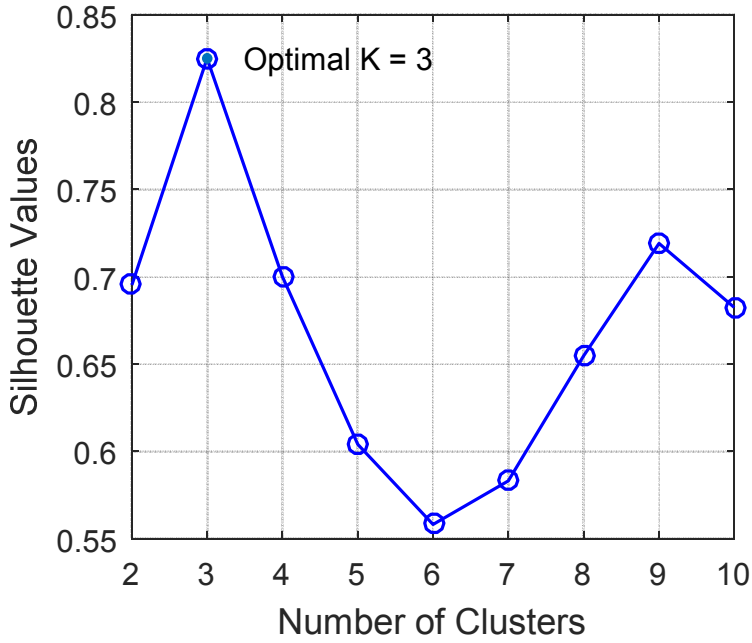

Figure 4: Mean silhouette value criterion for cluster evaluation to optimize number of clusters for Haxby Road; *k*-means++ clustering algorithm has been applied.

Secondly, the agglomerative hierarchical cluster tree [7] algorithm was applied. This algorithm begins by considering each observation as a single cluster and combines two clusters to create a larger one at each step. The selection of the clusters to be combined is determined by a distance metric. The algorithm stops when the desired number of clusters is obtained. The steps of the algorithm are demonstrated in the resultant dendrogram shown in Figure 5. The process begins by considering 20 single-feeder clusters; the first step is to combine feeders 7 and 11; the second step combines 2 and 8; and the process continues until the desired number of clusters is acquired. Both algorithms resulted in the same clusters. We have employed two clustering algorithms to validate the results. However, the latter algorithm provides the user with enhanced insight in terms of linkages between feeders, i.e. similarity between feeders, and one can see all connections (i.e. steps of the algorithm) and are able to decide a different grouping of the observations if they want. For three clusters, the feeder groups are shown in blue, yellow, and red colour.

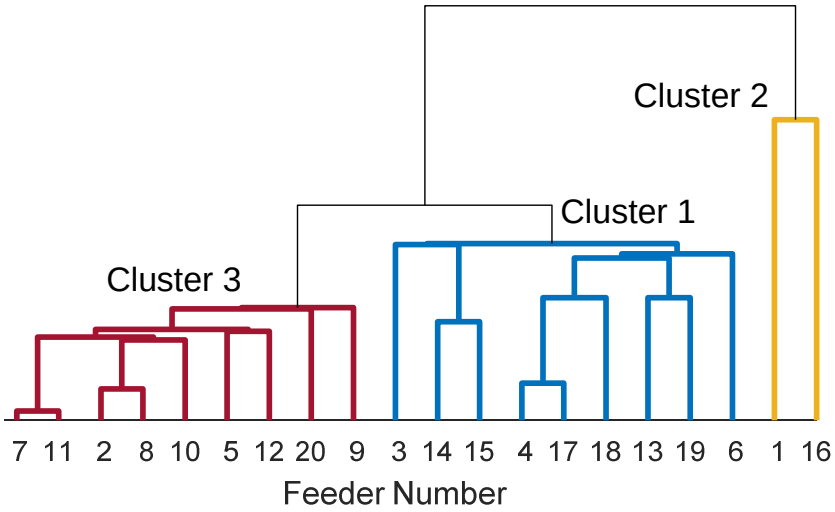

Figure 5: Dendrogram derived from the agglomerative hierarchical cluster tree algorithm for 7 Haxby Road and another 13 synthesized feeders based on the original ones.

2.4. Clustering Results

The results of the clustering process are shown in Table II. This table is essentially Table I in blue, yellow, and red colour in order to link each feeder to a cluster – the colours correspond to Figure 5.

Table II: Clustering results for the set of feeders shown in Table I. Rows in blue correspond to Cluster 1; yellow rows to Cluster 2; and red rows to Cluster 3.

Feeder Name-Number /Feature	Length of main feeder (km)	Length of laterals (km)	Number of laterals	Resistance of main feeder (pu)	Resistance of laterals (pu)	Peak Demand (MW)	Number of load points	Load Factor	Load Distribution Factor
Bumper Castle (1)	7.667	3.585	6	1.25	0.818	2.2958	19	0.4848	0.7744
Haxby R. H. (2)	1.402	0	0	0.18	0	0.508	3	0.5285	0.9082
Bowl. Green Ct (3)	8.01	0.72	2	1.2	0.136	1.8363	9	0.4861	0.7214
New Earswick (4)	6.057	1.262	2	1.146	0.38	2.022	10	0.516	0.6137
Kirkham Ave. (5)	1.992	0.359	1	0.244	0.049	0.6959	4	0.367	0.61
Hambleton Tce (6)	3.636	1.23	2	0.44	0.148	3.4062	9	0.3417	0.525
Fossway (7)	0.658	0	0	0.144	0	0.8057	2	0.3408	0.6464
Synth.Feeders									
(8)	1	0	0	0.16	0	0.45	3	0.32	0.65
(9)	2	0	0	0.35	0	1.75	5	0.45	0.55
(10)	1.5	0	0	0.28	0	0.75	4	0.34	0.62
(11)	0.7	0	0	0.1	0	0.7	2	0.53	0.7
(12)	2.5	0.4	1	0.375	0.08	0.9	5	0.47	0.71
(13)	5	0.7	2	0.8	0.15	1.5	8	0.5	0.65
(14)	7.5	1.2	3	0.975	0.252	2.4	12	0.54	0.68
(15)	8	1	3	1.36	0.19	1.98	11	0.37	0.72
(16)	9	1.4	4	1.44	0.21	2.55	17	0.39	0.74
(17)	6	0.85	2	0.96	0.255	2.1	10	0.48	0.69
(18)	4.5	0.72	2	0.585	0.1656	1.8	10	0.34	0.6
(19)	3.5	0.6	2	0.42	0.15	1.2	8	0.52	0.54
(20)	2	0.33	1	0.38	0.0627	1.8	6	0.48	0.63

It can be seen in figure 5 and table II that Cluster 2 contains two of the longest feeders which also have the greatest number of laterals as well as number of load points. Cluster 1 consists of nine feeders which have lengths varying from 3.5 – 8 km with mainly two laterals

and about 10 load points. Finally, Cluster 3 comprises the remaining nine feeders which are 0.7 – 2.5 km long with zero or one laterals, 2-6 load points, and 0.45-1.8 MW load.

Now, having clustered the feeders, we can produce the representative (or mean) feeder for each cluster; we do so by calculating the mean value of each characteristic for all feeders within the cluster. The three representative feeders are presented in Table III below. Figure 6 illustrates the representative feeder of Cluster 1, each load point of which is 2.03/10 = 0.203MW; the resistance of each main feeder section is equal to 0.876/10 = 0.0876 pu; and the resistance of each lateral is 0.203/2 = 0.105 pu. Laterals are evenly distributed across the feeder, and one load point is assigned to each lateral, otherwise, a lateral section would not supply any load. The representative feeders for Clusters 2 and 3 can be constructed following the same approach (see Figure *32* in the Appendix).

Table III: Representative feeders for each cluster (for the aforementioned set of 20 feeders).

Cluster	Length of main feeder (km)	Length of laterals (km)	Number of laterals	Resistance of main feeder (pu)	Resistance of laterals (pu)	Peak Demand (MW)	Number of load points
1	5.8	0.92	2	0.876	0.203	2.03	10
2	8.33	2.49	5	1.345	0.514	2.42	18
3	1.53	0.12	0	0.246	0.021	0.93	4

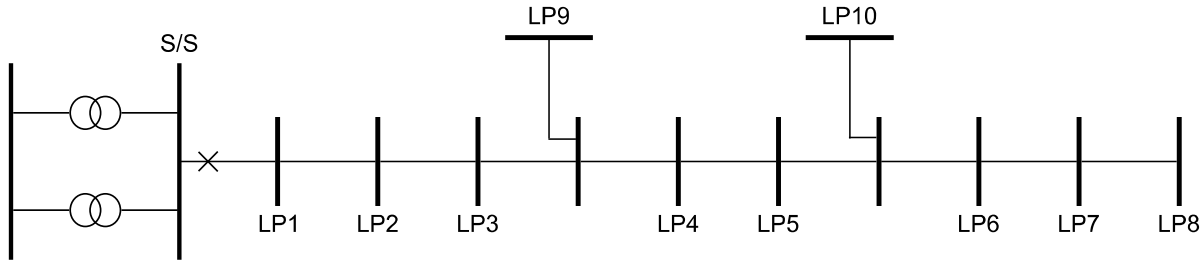

Figure 6: Representative feeder of Cluster 1.

2.5. Estimation of Losses Based on the Representative Feeder

Having obtained the representative feeder for each cluster, we can calculate losses for each one. Based on the loss of the representative feeder, we can estimate losses for any feeder in the cluster as shown below:

$$Losses_{\text{feeder}} = Losses_{\text{rep.feeder}} \cdot a \tag{2.3}$$

where

$$a = \left(\frac{P_{\text{feeder}}}{P_{\text{rep.feeder}}} \right)^2 \cdot \left(\frac{\sum_i PL_{i,\text{feeder}}}{\sum_i PL_{i,\text{rep.feeder}}} \right)^2 \tag{2.4}$$

where P refers to power; L to distance; and i is the load point index.

In equation (2.3), a is called modifier and is associated with the load and LDF of the feeder and the corresponding values of the representative feeder. Table IV presents the estimated losses for the three real feeders of Haxby network. Results are satisfactory (<10% according to [1]) for two of them, but for the third we have a significant error. This feeder has considerably higher (68% of the peak demand of the representative feeder) loading than the rest of the feeders, which has as a result an over-adjustment when the modifier is applied on the loss of the representative feeder. The representative feeder does not capture each feeder of the cluster perfectly. Hambleton Terrace feeder is considered an outlier because of its peak demand; its other characteristics are in accordance with the rest of the feeders in the cluster.

Table IV: Feeder losses at peak demand for Cluster 1.

Feeder	Actual Losses (kW)	Estimated Losses (kW)	Relative Error (%)
Representative	15.09	–	–
Bowling Green Court	30.12	31.05	3.09
New Earswick	20.13	18.89	6.16
Hambleton Terrace	24.71	40.11	62.32

2.6. Summary

This section presented a feeder clustering process based on nine characteristics that are considered relevant to losses. The proposed approach is generic (i.e. does not depend on specific networks) and fits with the literature. The aim is to obtain a representative feeder for each cluster; calculate losses for each one; and then based on the loss of the representative feeder, derive losses for any other feeder within the cluster using the above-mentioned modifier. We applied this method on a set of 20 feeders, of which seven were real (Haxby primary) and 13 synthesized. The proposed method produced a satisfactory estimation (<10%) for two of the real feeders and yielded a considerable error for the third one; the loading of this feeder, however, was significantly higher (68%) than the rest of the feeders in the cluster (outlier). The proposed method has performed well on the aforementioned dataset; in order to increase confidence, we propose its application to a larger set of real feeders.

3. Network Reconfiguration

3.1. Introduction

This section examines network reconfiguration which can be defined as changing the topology of the network by opening and closing line switches [8]. The goal of network reconfiguration is to find a radial configuration which minimizes a specific objective function

[9]. Losses, load balancing, voltage deviation, and reliability have been commonly used as objective functions in relevant studies [8]. This section considers losses and reliability optimization on one of the UK Generic Distribution Systems (UKGDS).

3.2. Description of Case Study Network

The case study network is presented in Figure 7; this is the HV UG UKGDS [10]. The high-level characteristics of the network are listed below:

1) Urban area.
2) Short feeder length.
3) High customer density.
4) Underground (UG) construction.
5) Radial topology.
6) Small overall size.

The network consists of 76 buses (at 11 kV) and 75 branches without considering normally open points (NOPs). In terms of demand, there are 75 load point which account for 24.27 MW and 4.85 MVAr. Minimum voltage is at bus 75 (endpoint of feeder 8) equal to 0.948 pu considering substation voltage 1.0 pu. Power losses for the original configuration are 431 kW.

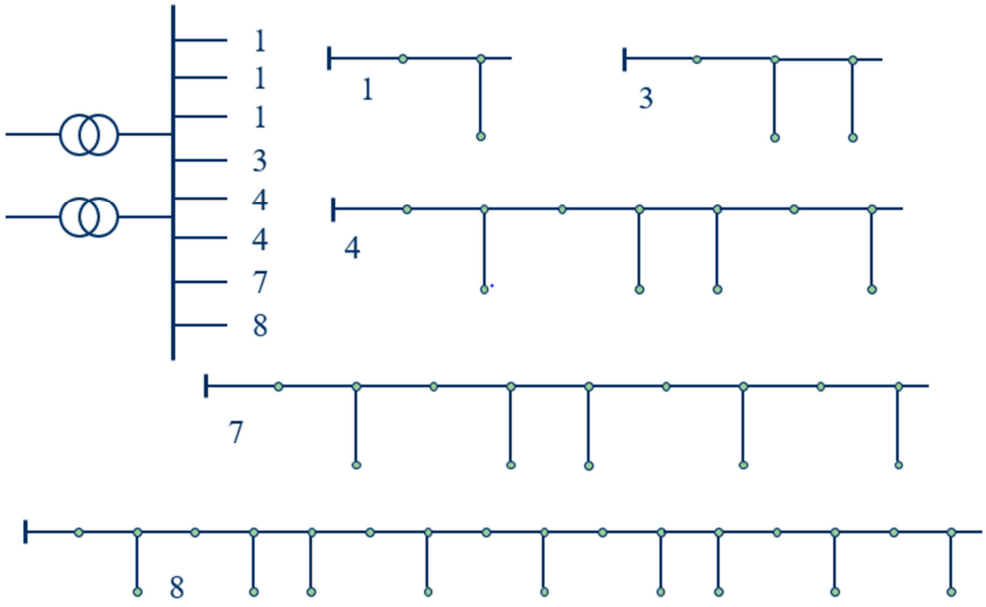

Figure 7: HV UG UKGDS [10].

As there were no NOPs in the original network, we considered seven interconnections between feeders, based on a typical urban Northern Powergrid (NPg) distribution network such as Haxby primary. The eight feeders of the network with bus numbers are shown in

Figure 8 and the considered NOPs in Table V. Four of the NOPs (1-4) connect the feeder endpoints, specifically: F1-F8, F2-F7, F3-F6, and F4-F5. There are another two NOPs (5 and 7) which connect the midpoints of the longer feeders, i.e. F5-F6 and F7-F8. The last NOP (6) provides another interconnection between F6 and F7. The network with the normally open points is illustrated in Figure 33 (in the Appendix).

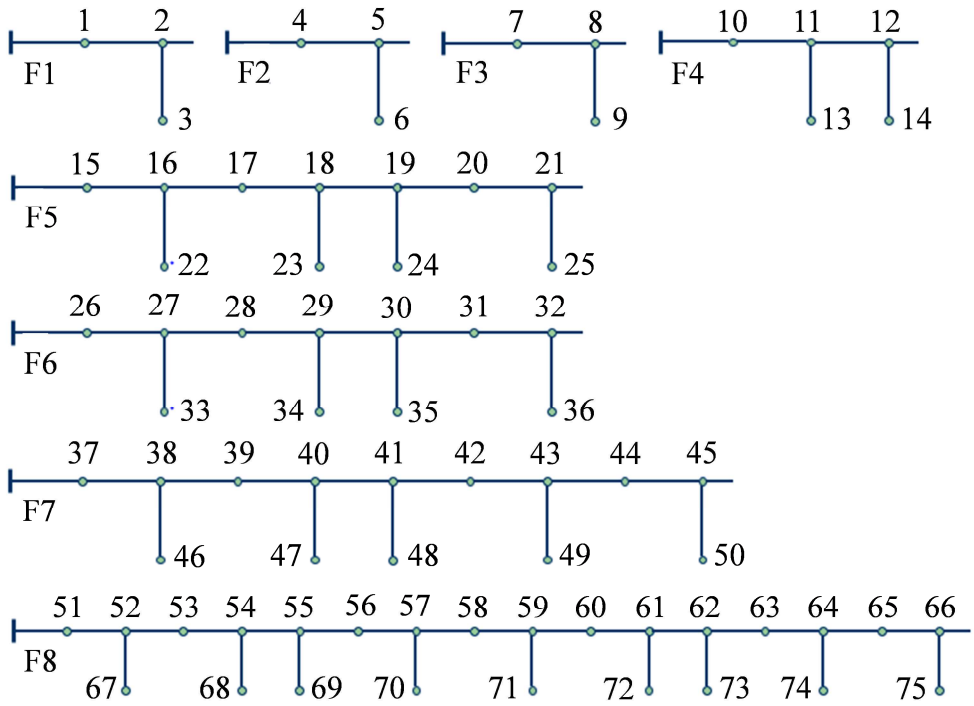

Figure 8: All eight feeders of HV UG UKGDS with bus numbers.

Table V: Considered NOPs for the HV UG UKGDS network.

NOP	Interconnecting Buses	Interconnecting Feeders	Branch Number
1	2-66	F1-F8	76
2	5-45	F2-F7	77
3	8-32	F3-F6	78
4	12-21	F4-F5	79
5	18-29	F5-F6	80
6	31-38	F6-F7	81
7	41-59	F7-F8	82

3.3. Minimum Loss Reconfiguration (Single-Time Step Simulation)

The number of possible radial configurations for the network above is ~5.78 million, according to Kirchhoff's matrix-tree theorem [11]; some of them might violate thermal or voltage limits. This demonstrates the need for optimization problem formulation. We formulate the problem based on [8]; the authors in this paper optimize network configuration considering network losses and reliability (in terms of expected customer interruption cost) whilst accounting for asset condition and substation reliability. In this report, we consider

minimization of losses as the sole objective, and we solve the model using Genetic Algorithm, which has been widely used in the relevant literature (e.g. [12-14]). Power losses for the original and optimal network configurations (illustrated in Figure 33 and Figure 34 in the Appendix) are shown in Table VI; there is a significant reduction of ~40% in losses. Each radial configuration can be represented in terms of open branches; a necessary but not sufficient condition is that the number of the closed branches should be equal to $N_b - 1$, where N_b is the number of buses of the network. In this case study, we have 75 branches of the original network and 7 NOPs; therefore, we need 7 branches to be open. Branch 1-2 corresponds to branch number 2, branch 2-3 to branch number 3, etc.

Table VI: Power losses for the original and optimal network configurations.

Configuration	Open Branches	Losses (kW)
Original	76, 77, 78, 79, 80, 81, 82	431.0
Optimal	62, 42, 31, 79, 80, 81, 59	259.7 (-40%)

After reconfiguration, the voltage profile of the network as well as the loading of each feeder has been significantly improved. This is primarily because heavily loaded feeders can transfer load to feeders which supply fewer load points and are more lightly loaded. Load balance between feeders improves losses and voltage. This is illustrated in Figure 9 and Figure 10. Feeder F5 (11 load points) does not transfer any load to feeder F4 (5 load points) because the main feeder sections of the latter have a resistance approximately 3.5 times higher than that of the former. Consequently, feeders F4 and F5 are balanced in terms of losses in the original configuration, and load transfer between them is not required.

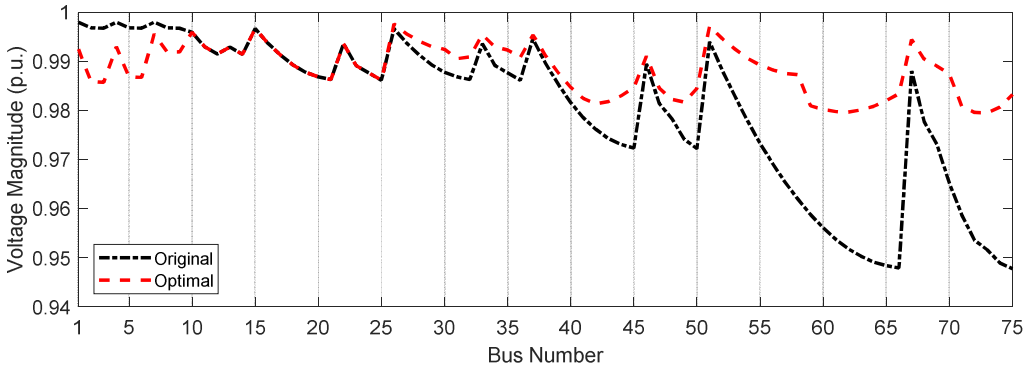

Figure 9: Voltage profile for original and optimal network configurations for the HV UG UKGDS network.

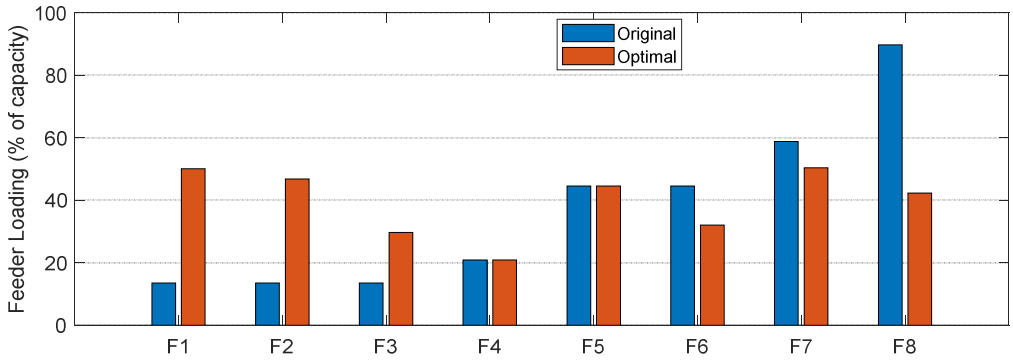

Figure 10: Feeder loading for original and optimal network configurations for the HV UG UKGDS network.

3.4. Reliability Reconfiguration

This section optimizes the configuration of the network for reliability; System Average Interruption Duration Index[1] (SAIDI) is considered as the objective function. This index accounts for both frequency and duration of failures, and considers number of customers lost rather than energy not supplied. The optimization of this index will therefore balance number of customers between feeders. Intuitively speaking, the longer the feeder, the greater the impact of each single feeder section failure, and when it occurs, the greater the number of disconnected customers. Whereas, when customers are better distributed between the feeders, then feeder failures affect a smaller part of the healthy network, and fewer customers are interrupted. If specific feeder sections are quantifiably less reliable, it may be optimal to transfer customers away from these even if it results in a less balanced network.

Based on [15, 16], we consider a switching time of 15 min (remote control) and a repair time of 5 hours; a failure rate of 0.065 f/yr·km; 2.5 kW / residential customer and 41.5 kW / commercial customer have also been assumed (see Table XIV in the Appendix for customer types). The number of customers supplied by this network is 5,492. SAIDI reconfiguration results are shown in Table VII.

Table VII: SAIDI for the original and optimal network configurations.

Configuration	Open Branches	SAIDI (hr/cust·yr)	CML* (min/100 cust·yr)
Original	76, 77, 78, 79, 80, 81, 82	0.1628	97.68
Optimal	61, 42, 30, 21, 80, 81, 59	0.1249 (-23%)	74.94

*CML = Customer Minutes Lost.

[1] SAIDI is the average outage duration for each customer served and is calculated as the sum of all customer interruption durations divided by the number of customers served.

3.5. Multi-Objective Reconfiguration

Having separately presented networks with minimised losses and minimised SAIDI reconfiguration, we now formulate a multi-objective optimization problem to consider both objectives simultaneously. The output of this model is the Pareto front which is illustrated in Figure 11. Pareto optimality is a state where it is impossible to further improve one objective function without deteriorating the other. In other words, for each point on the Pareto front of Figure 11, we can improve one objective function only by degrading the other [17]. When a Pareto front is obtained, then the decision maker can apply different weights (depending on their preferences) on the objectives and select the one with the best overall performance. In this case study, we observe that we can get low values for both objectives simultaneously; this demonstrates that the objectives do not compete each other in this case study. Note that power loss and SAIDI for the original configuration are 431 kW and 0.1628 hr/cust·yr.

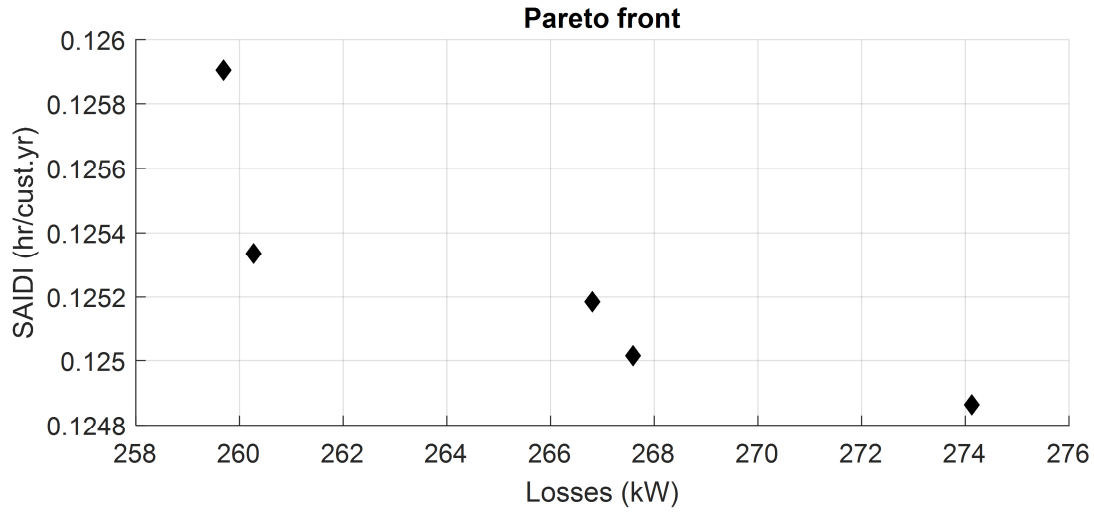

Figure 11: Pareto front for multi-objective network reconfiguration considering power losses and SAIDI.

3.6. Minimum Loss Reconfiguration (Multi-Time Step Simulation)

So far, we have examined network reconfiguration for a single time step (i.e. finding the optimal configuration for a specific loading condition – usually at peak load). In this section, we present a multi-time step analysis for the minimum loss reconfiguration problem. This means that we optimize the configuration of the network each time step (here one hour) accounting for the variability of demand. Generally, multi-time step (here hourly) reconfiguration provides improved results at the cost of performing multiple switching actions to change between different network configurations throughout the day. Demand profiles for each customer type are taken from [18] (see Table XIV in the Appendix for customer types). Power losses for each hour for: a) fixed original configuration; b) fixed

optimal configuration (derived in Section 3.3 and corresponds to the green configuration in Table IX); and c) hourly optimal configuration, are presented in Figure 12. To further clarify, configuration (a) refers to the original network configuration (illustrated in Figure 33 in the Appendix), i.e. with branches 2-66, 5-45, 8-32, 12-21, 18-29, 31-38, and 41-59 (which correspond to the considered NOPs) open. In this case, the original configuration is kept fixed during the day and losses are calculated every hour considering this configuration. Configuration (b) refers to the optimal configuration obtained in Section 3.3, which corresponds to a specific loading condition of the network given in [10]; this configuration is illustrated in Figure 34 in the Appendix. Finally, configuration (c) is the optimal configuration for each hour, i.e. the network configuration given by the optimization algorithm, which is run at each time step considering variable demand profiles. The corresponding energy losses throughout the day are shown in Table VIII. Table IX shows the hourly optimal configuration (case c) for each time step. We observe the following:

1) Fixed optimal (b) and hourly optimal (c) both achieve approximately 40% reduction in daily energy losses. The difference between (b) and (c) is negligible (0.33%).
2) There are only three different configurations f
3) or (c) (shown in different colours), which are also quite similar to each other; there are 2-3 different open branches between the different configurations.
4) Two of the NOPs (18-29 and 31-38) were not operated, i.e. remained open for all 24 hours of the day.
5) Four open branches (including the two above-mentioned NOPs) remained unchanged throughout the day. This is indicative of the similarity between the different configurations obtained by the optimization algorithm for each time step.

These findings suggest the use of fixed optimal configuration (b) during the day, since hourly optimal configuration (c) requires five configuration changes throughout the day (see Table IX) and only offers an extra 0.33% improvement in losses. In addition, fixed optimal configuration (b) (shown in green in Table IX) is optimal for 15 out of the total 24 hours.

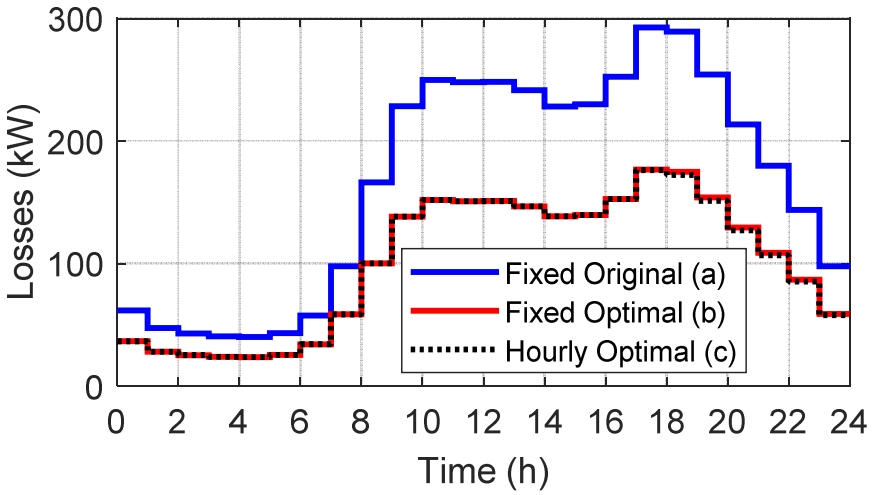

Figure 12: Power losses for each hour for: a) fixed original, b) fixed optimal, and c) hourly optimal configurations.

Table VIII: Daily energy losses for: a) fixed original, b) fixed optimal, and c) hourly optimal configurations.

Configuration	Energy Losses (MWh)
Fixed Original (a)	3.996
Fixed Optimal (b)	2.4147 (-39.57%)
Hourly Optimal (c)	2.402 (-39.9%)

Table IX: Optimal configuration for each time step for case c (hourly optimal configuration). Different colours are used to indicate different network configurations. There are three different configurations throughout the day, and five changes between different configurations.

Time	Configuration						
1	62	43	32	21	80	81	59
2	62	42	31	79	80	81	59
3	62	42	31	79	80	81	59
4	62	42	31	79	80	81	59
5	62	42	31	79	80	81	59
6	62	42	31	79	80	81	59
7	62	42	31	79	80	81	59
8	62	42	32	21	80	81	59
9	62	42	31	79	80	81	59
10	62	42	31	79	80	81	59
11	62	42	31	79	80	81	59
12	62	42	31	79	80	81	59
13	62	42	31	79	80	81	59
14	62	42	31	79	80	81	59
15	62	42	31	79	80	81	59
16	62	42	31	79	80	81	59
17	62	42	31	79	80	81	59
18	62	42	32	21	80	81	59
19	62	43	32	21	80	81	59
20	62	43	32	21	80	81	59
21	62	43	32	21	80	81	59
22	62	43	32	21	80	81	59
23	62	43	32	21	80	81	59
24	62	43	32	21	80	81	59

3.7. Summary

The findings demonstrate that network reconfiguration can significantly improve power losses and reliability. Case study results showed a reduction of approximately 40% in losses and 23% in SAIDI. Multi-objective optimization indicated that both objectives can take very high-quality values (i.e. very close to the single-objective optimal) simultaneously. This fact shows that power losses and SAIDI – to a large extent – work synergistically, i.e. when one objective improves, the other improves as well (in this case study). However, this depends on customer types, demand profiles, and customer distribution between the feeders. Finally, hourly network reconfiguration – compared to fixed optimal configuration – provides an additional improvement of 0.33%, which can be considered negligible.

4. Soft Open Points

4.1. Introduction

Soft open points (SOPs) are power electronic devices which are used to interconnect two (or more) feeders in place of normally open points (see Figure 13) [19]. Two important characteristics of SOPs are [20]:

1) The ability to continuously control active power flow between the interconnected feeders.
2) The capability to inject/absorb reactive power independently at the AC terminal nodes.

These characteristics can significantly influence the optimal operation and planning of modern distribution networks.

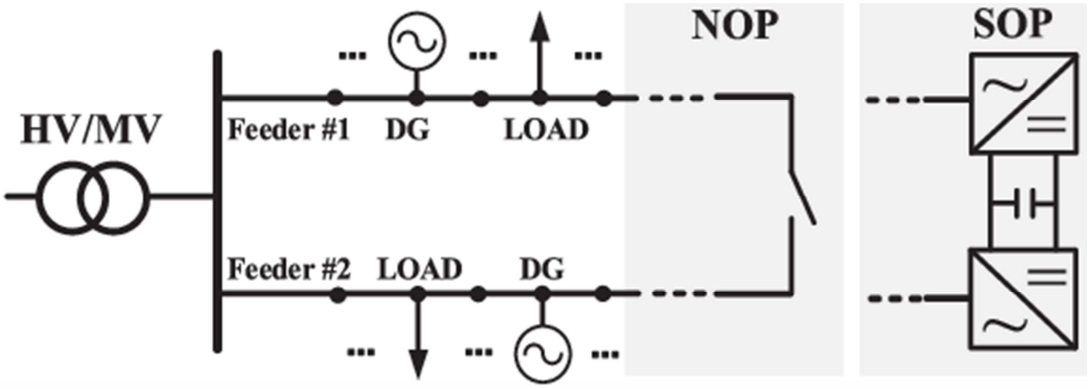

Figure 13: Schematic of SOP installation [21].

4.2. Case Study Network

The case study network consists of feeders F1 and F8 of the HV UG UKGDS (see Figure 8) connected via an SOP, and is presented in Figure 14 below. The network supplies 28 load points with a total active demand of 8.41 MW and a total reactive demand equal to 1.68 MVAr. Power losses for the original configuration and the optimal reconfiguration (without SOPs) are provided in Table X for benchmarking purposes.

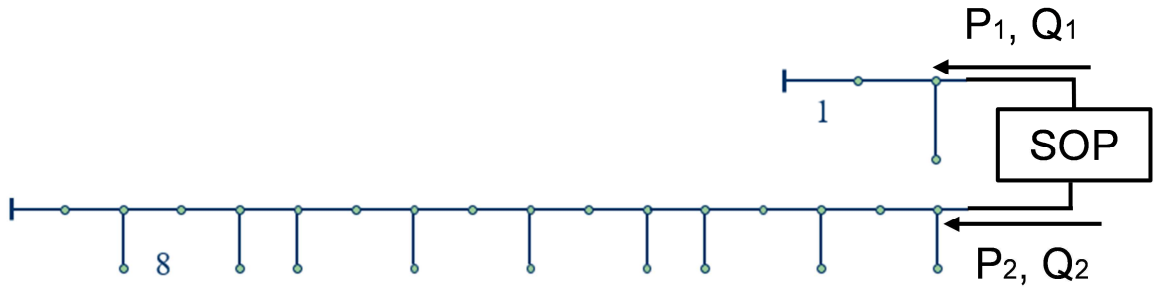

Figure 14: Case study network: F1 and F8 of the HV UG UKGDS interconnected through an SOP.

Table X: Power losses for the original configuration and the optimal reconfiguration (for comparison – no SOP).

Configuration	Power Loss (kW)
Original	257
Optimal	133.9 (-47.9%)

4.3. SOP Model

According to [22], the power balance for a SOP is described as

$$P_1 + P_2 + A_1|P_1| + A_2|P_2| = 0 \tag{4.1}$$

where P_1, P_2 are the active power injections at the endpoints of feeders F1 and F8, respectively; and A_1, A_2 are the converter loss coefficients.

Equation (4.1) expresses the active power balance of the device, as the active power injections are not independent to each other. If loading is reduced on one feeder, then it will be increased on the other. Conversely, reactive power injections are independent of each other, i.e. Q_1, Q_2 independent. However, SOP capacity constraints should be satisfied at both sides. This is expressed through (4.2) and (4.3) and is illustrated in Figure 15.

$$\sqrt{P_1^2 + Q_1^2} \leq S_1 \tag{4.2}$$

$$\sqrt{P_2^2 + Q_2^2} \leq S_2 \tag{4.3}$$

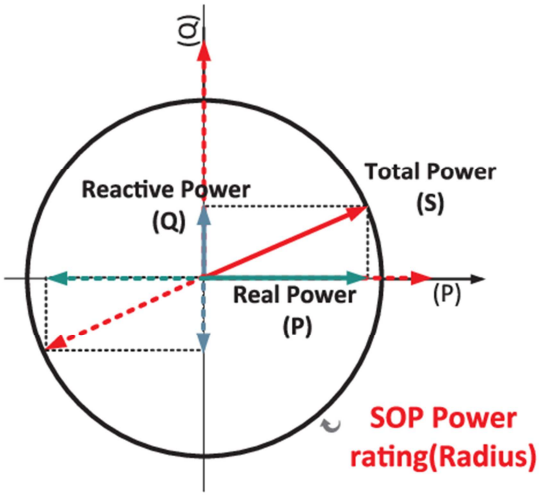

Figure 15: Operating region for Voltage Source Converter (VSC) based SOP in *P*-*Q* plane [23].

4.4. SOP Optimization

This section performs SOP optimization with the aim to minimize network losses. The problem is mathematically formulated as a second order cone programming (SOCP) model, which guarantees global optimality and computational efficiency using commercial solvers, such as Gurobi [24], MOSEK [25], and CPLEX [26]. The following two subsections examine the impact of: 1) SOP rating; and 2) SOP efficiency, on network losses.

4.4.1. SOP Rating

The effect of SOP rating (varying from 1-3 MVA) on network losses is analysed in this subsection. These ratings are generic for SOPs at 11 kV, as the authors in [19]-[21] consider SOP ratings from 0.5-3 MVA at voltage levels, ranging from 12.66-20 kV. SOP is assumed to be lossless here, i.e. $A_1 = A_2 = 0$. SOP optimization results are presented in Table XI. The lowest power loss (for a 3-MVA SOP) is 123.3 kW, which corresponds to a reduction of 52% compared to the original configuration (257 kW). It can be seen that while for ratings of 1 MVA and 2 MVA, the SOP if fully utilized, for a rating of 3 MVA, the converters do not operate at their rated capacity. This is because the load transfer from the heavily loaded feeder F8 to the lightly loaded feeder F1 has reached a limit beyond which losses start to increase. The load transfer is implemented through active power injections P_1 and P_2. P_2 is a positive injection (equivalent to generation) at the end of feeder F8; P_1 is a negative injection (equivalent to load) at the end of feeder F1. The reactive power injections Q_1 and Q_2 are both positive (equivalent to generation); SOPs can inject (or absorb) reactive power independently at both sides [20]. Reactive power primarily supports voltage, but also losses because it reduces the current that flows from the substation through the feeders. Compared to optimal

network reconfiguration (-47.9%), an SOP would achieve lower power loss, if it had a rating greater than approximately 2 MVA (-47.5%).

Table XI: SOP optimization results for various SOP rating values ($A_1 = A_2 = 0$ – lossless SOP).

Rating (MVA)	Losses (kW)	$-P_1 = P_2$ (MW)	Q_1 (MVAr)	Q_2 (MVAr)	S_2 (MVA)
1	178.7 (-30.5%)	0.971	0.1453	0.2391	1
2	135.0 (-47.5%)	1.93	0.1544	0.5226	2
3	123.3 (-52%)	2.7472	0.1649	0.8297	2.87

Figure 16 illustrates the loss reduction versus SOP rating. As was mentioned earlier, there is a point for the load transfer between the feeders, beyond which losses no longer decrease. This point is when there is load balance between the feeders; the greater the imbalance, the more SOP can contribute towards loss reduction. Beyond this point, an imbalance would occur again, but now the initially lightly loaded feeder would become more heavily loaded (i.e. in this case study feeder F1 would become more heavily loaded than feeder F8). Therefore optimization stops at this point, and loss reduction reaches this plateau. This finding can be generalized to any pair of feeders.

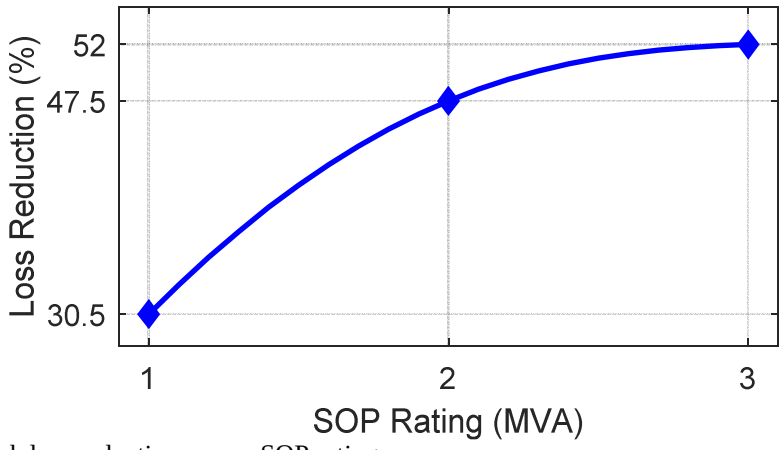

Figure 16: Network loss reduction versus SOP rating.

4.4.2. SOP Efficiency

The value of loss coefficients of power converters is varied to examine the impact on network losses in this subsection. SOP rating is considered fixed at 2 MVA. Table XII shows the corresponding results. Power losses increase (from 135 kW up to 150.8 kW) as the value of loss coefficients rises (from zero to 10%). Note that while the active power injection P_1 remains around a value very close to -2 MW (equivalent to an additional load of 2 MW at the end of feeder F1), the value of active power injection P_2 keeps decreasing. This means that load reduction at feeder F8 falls as loss coefficients increase, which causes network losses to increase as well.

Table XII: SOP optimization results for different efficiencies (SOP rating fixed at 2 MVA).

$A_1 = A_2$	Losses (kW)	P_1 (MW)	Q_1 (MVAr)	P_2 (MW)	Q_2 (MVAr)
0	135.0 (-47.5%)	-1.93	0.1544	1.93	0.5226
0.02	136.8 (-46.8%)	-1.9968	0.1125	1.9185	0.565
0.05	141.5 (-44.9%)	-1.9991	0.0605	1.8087	0.75
0.1	150.8 (-41.3%)	-1.999	0.0634	1.6355	0.8759

4.5. Summary

Section 4 presented Soft Open Points, their modelling, and optimization to minimize network losses. A case study network of two interconnected feeders via an SOP was considered. Power loss for the original network configuration was 257 kW, whereas for optimal reconfiguration 133.9 kW, which corresponds to a reduction of 47.9%. Various SOP rating and loss coefficients were used to study their impact on network losses. A 1-MVA SOP managed to reduce losses by 30.5%, while a 3-MVA SOP achieved the maximum reduction (52%) in this case study (considering zero loss coefficients). When SOP losses are incorporated in the model, network loss reduction is lower; the increase in losses compared to the lossless model can be up to 6% (considering a loss coefficient per converter ranging from zero to 10%). Finally, in terms of loss reduction, SOP (a maximum of 52% at 3 MVA) and network reconfiguration (~48%) achieve comparable results, with SOP having slightly better performance for a rating greater than 2 MVA.

5. Electric Vehicles (EVs)

5.1. Case Study

5.2.1. Network and Data

Feeder F8 of the HV UG UKGDS (see Figure 8) is used in this case study, and is illustrated in Figure 17. This feeder supplies 25 load points with a total active demand of 7.51 MW and total reactive demand of 1.5 MVAr. If the substation voltage is 1.05 pu then the minimum voltage is 1.0 pu. The thermal limit for main feeder sections is 8.86 MVA.

Figure 17: Case study network. Feeder F8 of the HV UG UKGDS.

We consider multiple EVs – each with a maximum charging / discharging power of 7 kW and an energy capacity of 24 kWh – at every bus of the network, and with Vehicle to Grid (V2G) chargers. EVs are assumed to be unavailable from 8am – 6pm because they are being

used for commuting or other travel. The price profile used in this study is shown in Figure 18 [27] and the feeder demand without EVs is shown in Figure 19.

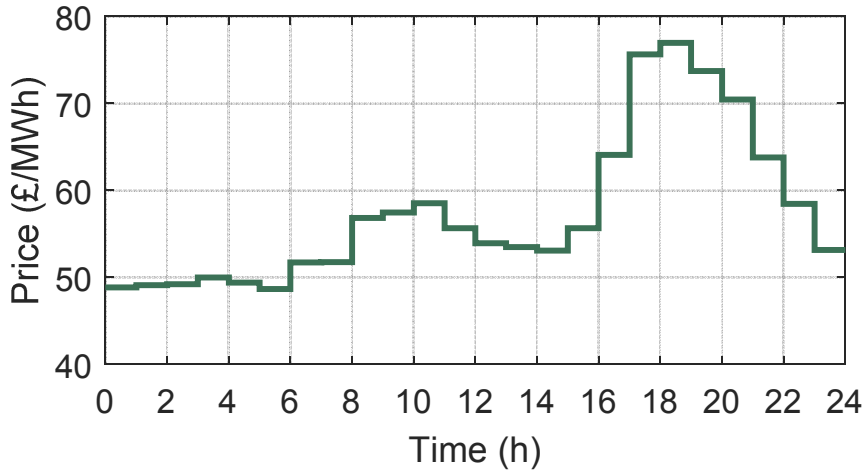

Figure 18: Price profile corresponding to a winner weekday taken from [27].

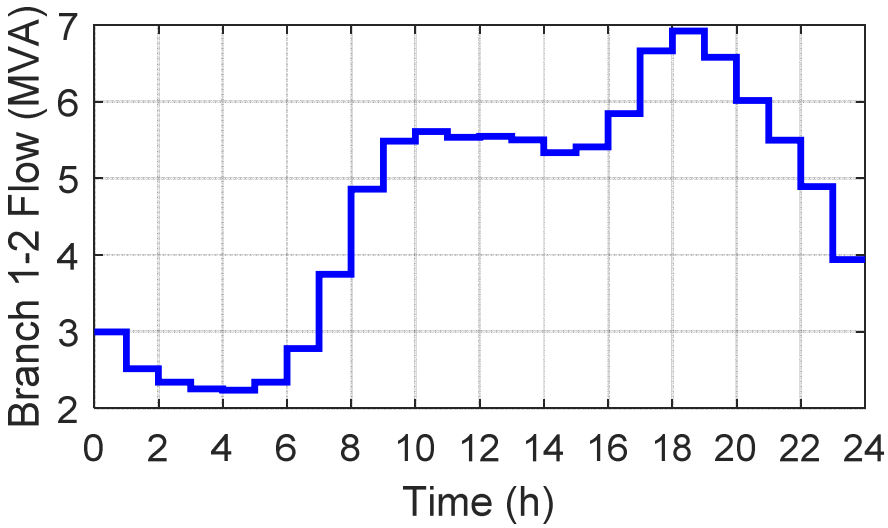

Figure 19: Feeder demand without EVs.

5.2.2. Test Case 1 (No Thermal Limits)

The aim of this study is to find the maximum number of EVs that can be hosted by a distribution feeder. The first test case neglects the thermal limits of the lines, and considers 1,071 EVs evenly distributed along the feeder. This number was chosen as a starting point for our study to ensure that we will have a thermal limit violation, if we ignore these constraints in the optimization. The objective function which determines the charging schedules of the EVs accounts for arbitrage profit only (in this test case), i.e.

$$\max \sum_{t} \left(P_{dch}(t) - P_{ch}(t) \right) \cdot p(t) \tag{5.1}$$

where P_{ch}, P_{dch} is the charging / discharging power of the EVs, and p is the price. The resulting aggregated state of charge of the EVs is illustrated in Figure 20. The EVs are unavailable from 08:00 – 18:00, as they start going to work at 08:00 and return home at 18:00. The model accounts for the energy required to deliver the transport (i.e., the vehicles arrive home with much less energy than they set out with). To maximize its profit, the aggregator discharges any energy available in the EVs from 18:00 onwards, as price peaks at that time.

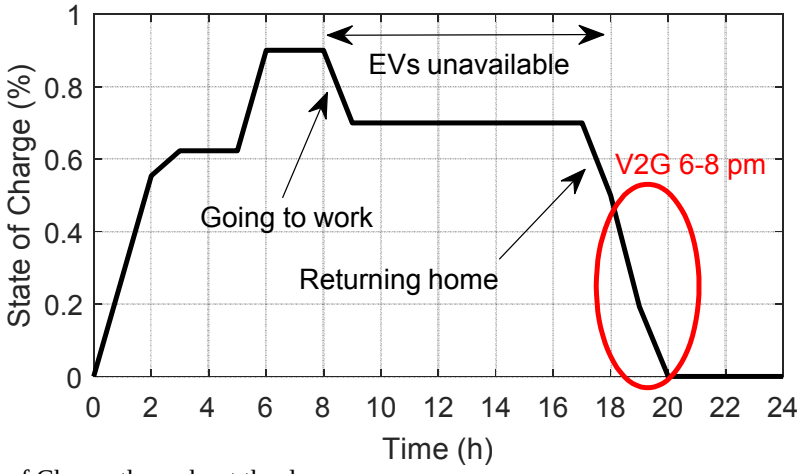

Figure 20: EV State of Charge throughout the day.

Charging and discharging schedule of the EVs is shown in Figure 21; charging takes place in the night when price is lowest, while discharging occurs from 18:00 – 20:00 when EVs are available and price is highest. Optimization is performed having the full price profile available. This means that the optimizer will choose these hours to charge, when price is the lowest, although price differences are very small. Any other charging profile would incur a greater cost. This situation should not be confused with real-time control, where a signal drives the EV power, in which case, it would be expected to see significant changes in the EV power as a result of considerable variations in the control signal.

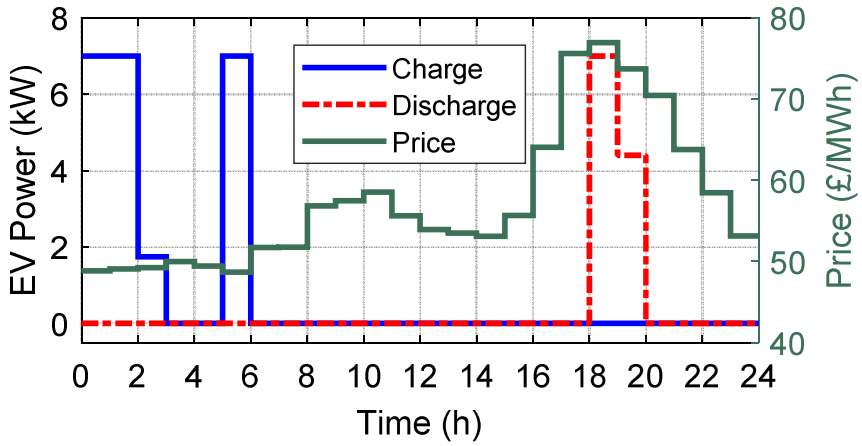

Figure 21: Charging / discharging schedule of EVs (objective: arbitrage profit only; thermal limits neglected).

Feeder demand in this test case is significantly different and exceeds the thermal limit – as shown in Figure 22 – which demonstrates that EV integration can substantially influence demand profile and impose heavy loading on a feeder (at different time of the day). This test case is used as a starting point for our case study and provides the direction for the following simulations.

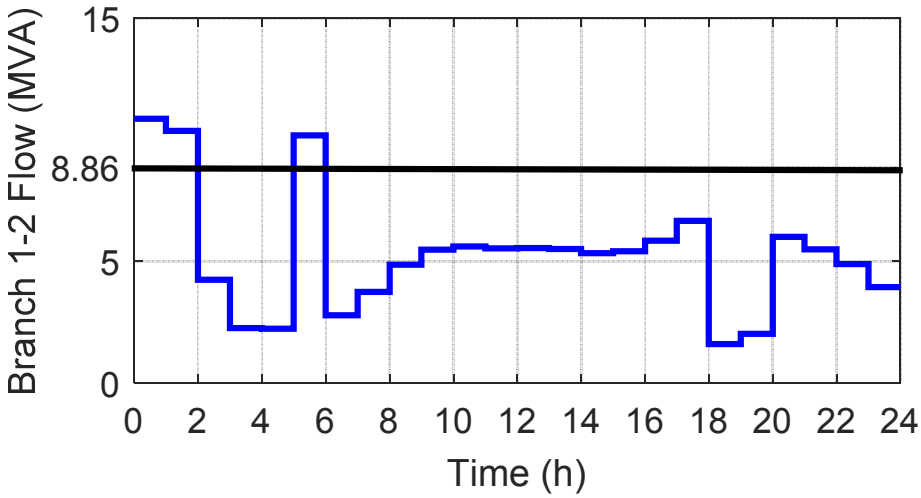

Figure 22: Feeder demand for Test Case 1 (with 1,071 EVs; neglecting thermal limits; and arbitrage profit only).

The next subsection considers thermal limits and investigates the impact of the incorporating network losses into the aggregator's decision-making via a signal provided by the DSO.

5.2.3. Test Case 2 (Thermal limits and Impact of Losses)

This subsection observes thermal limits and examines the impact of including network losses (by adding a weighted loss cost term) in aggregator's objective function (equation (5.2)).

$$\max \sum_t \left(\underbrace{\left(P_{dch}(t) - P_{ch}(t)\right) \cdot p(t)}_{\text{Arbitrage Profit } (t)} - \underbrace{w_L \cdot \text{Loss}(t) \cdot p(t)}_{\text{Weighted Loss Cost } (t)} \right) \tag{5.2}$$

Our aim is to find the maximum number of EVs which can be integrated in the network without exceeding thermal limits. Increasing the number of EVs, at some point, power flow will reach its limit at least for one hour during the day; this number constitutes the hosting capacity of EVs by the feeder. The number of EVs that can be hosted by the feeder – without thermal limit violation and without considering network losses (w_L = 0) in the decision-making of the aggregator – is 803. Feeder demand is illustrated in Figure 23 and the associated EV power per bus is shown in Figure 24. Feeder demand does not exceed the thermal limit in this test case; however, feeder loading is very close to its limit in the night when EVs are scheduled to charge. In addition, all EV schedules are identical because they all respond to the same price signal and the objective is only to maximize the arbitrage profit (see equation (5.1)). This simulation yields a minimum voltage of 0.946 pu (considering substation voltage = 1.05 pu). Daily energy loss is equal to 2.52 MWh, and cost of losses (calculated by multiplying the losses by the market price in each time step) is £142.

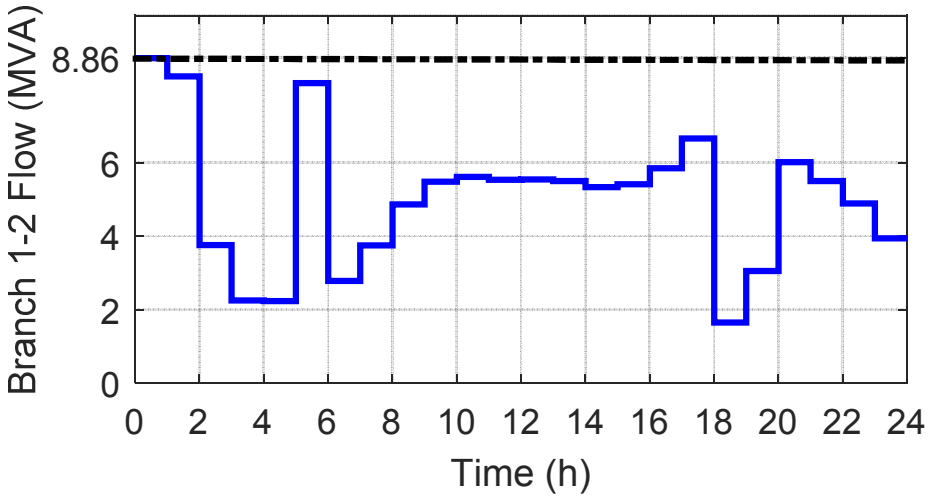

Figure 23: Feeder loading with 803 EVs; considering thermal limits; and not incorporating network losses into the objective function, i.e. w_L = 0.

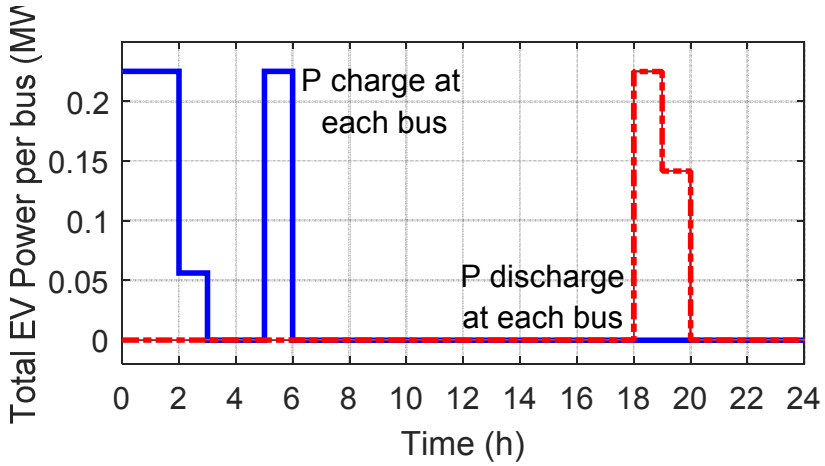

Figure 24: EV schedule (objective: arbitrage profit only, i.e. $w_L = 0$; thermal limits considered).

Next, we perform the same simulation, but with the incorporation of loss cost into the aggregator's objective function (with $w_L = 1$). Charging of the EVs has now been distributed more evenly over time during the night, which is caused by the inclusion of the losses term in the objective function (see (5.2)). This is illustrated in Figure 25. In the previous cases, the EV charging / discharging schedule was driven only by energy price, which led to simultaneous charging and discharging of the EVs to optimize cost (maximize profit); this means that all different charge and discharge lines in Figure 24 are on top of each other, appearing as single lines. Charge lines are no longer on top of each other in Figure 25, and this is why we can see all these lines in different colours. The avoidance of concurrent charging of all EVs during the night has caused a significant peak reduction, as shown in Figure 26. Voltage has also seen a major improvement, as minimum value now is 1.014 pu compared to 0.946 pu without considering network losses ($w_L = 0$). Energy loss is equal to 2.35 MWh (-6.75%), and cost of losses is £133.7 (-5.85%).

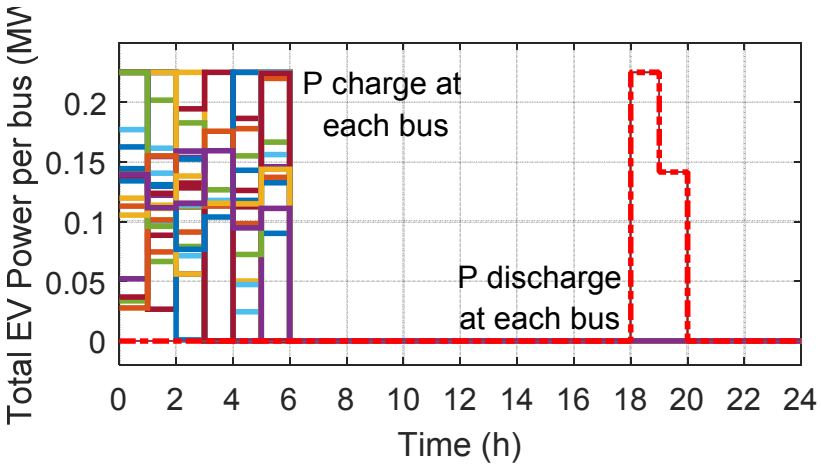

Figure 25: EV schedule (objective: arbitrage profit + loss cost, i.e. $w_L = 1$; thermal limits considered).

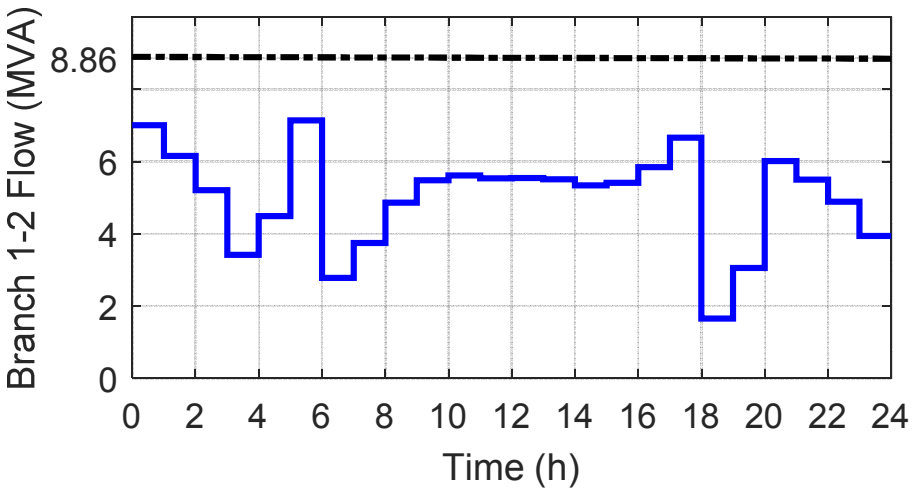

Figure 26: Feeder loading with 803 EVs; considering thermal limits; and incorporating network losses into the objective function with $w_L = 1$.

Figure 27 compares feeder demand for various values of w_L; the greater the value of w_L, the better the management of charging the EVs during the night, which results in lower peaks and improved voltage.

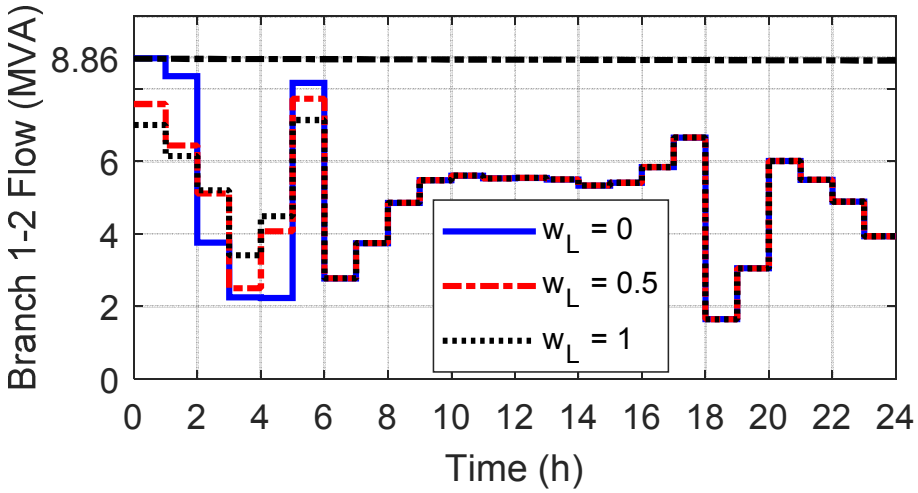

Figure 27: Feeder loading with 803 EVs; considering thermal limits; and incorporating network losses into the objective function with $w_L = 0$, 0.5, and 1.

Incorporating a cost of losses signal from the DSO into aggregator decision-making has led to an improved management of the EV fleet in terms of network utilization (lower peak and voltage improvement), which implies that the feeder can accommodate an increased number of EVs.

5.2.4. Test Case 3 (Thermal limits and Losses – Increased EV Hosting Capacity)

Having included loss cost in aggregator's objective function with $w_L = 1$, our aim is to find the new maximum number of EVs that can be accommodated by the feeder, while satisfying thermal and voltage limits. The maximum number of EVs is now 1,165 (+45%); the

associated feeder demand is illustrated in Figure 28. Minimum voltage is 1.01 pu (compared to 0.946 pu with w_L = 0 and 803 EVs). Energy loss is equal to 2.73 MWh (+8.3%), and cost of losses is £151.85 (+6.9%). Figure 29, shows the maximum number of EVs that can be hosted by the feeder versus w_L (the weighting factor for the cost of network losses paid by the aggregator).

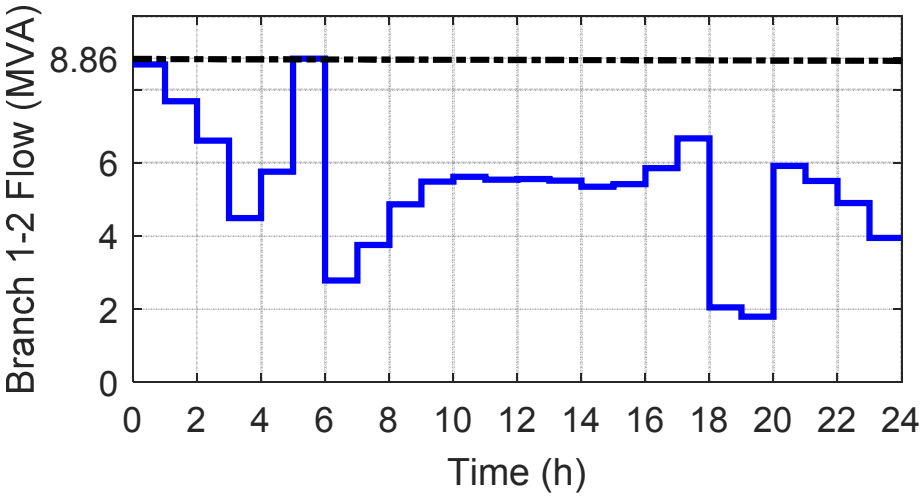

Figure 28: Feeder loading with 1,165 EVs; considering thermal limits; and incorporating network losses into the objective function with w_L = 1.

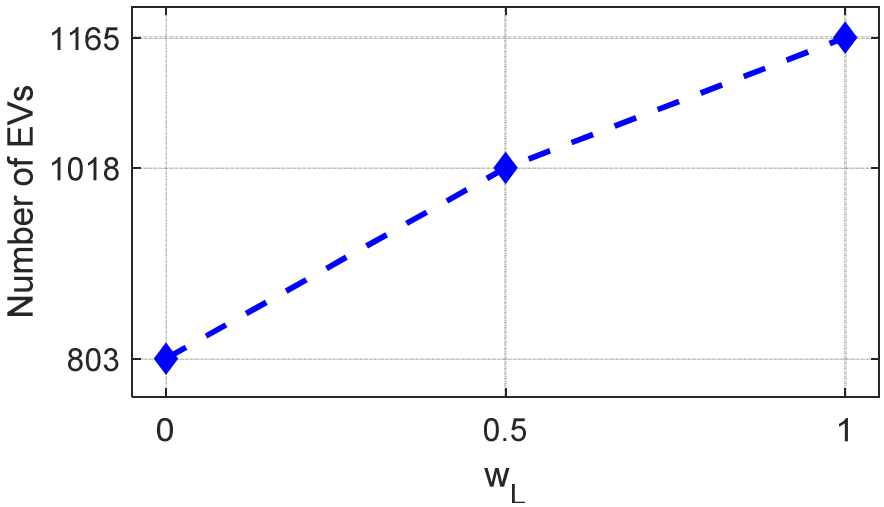

Figure 29: Maximum number of EVs that can be hosted by the feeder versus w_L.

5.2.5. Uncertainty and Probability of Violation

So far, we have not considered uncertainty in the case studies. To demonstrate the impact of uncertainty, we run 100 Monte Carlo simulations of Test Case 3 (with fixed EV schedules – obtained by optimization) considering a demand (including EVs) uncertainty of 10% (normal distribution). The results of these simulations are shown in Figure 30; it can be seen that a thermal limit violation has a considerable probability of occurrence. To evaluate the probability of violation (PoV), we run 10,000 Monte Carlo simulations, and for this case (w_L

= 1), we obtain a PoV of 45.31%. PoV can be managed by adjusting w_L; Table XIII shows the PoV for various w_L.

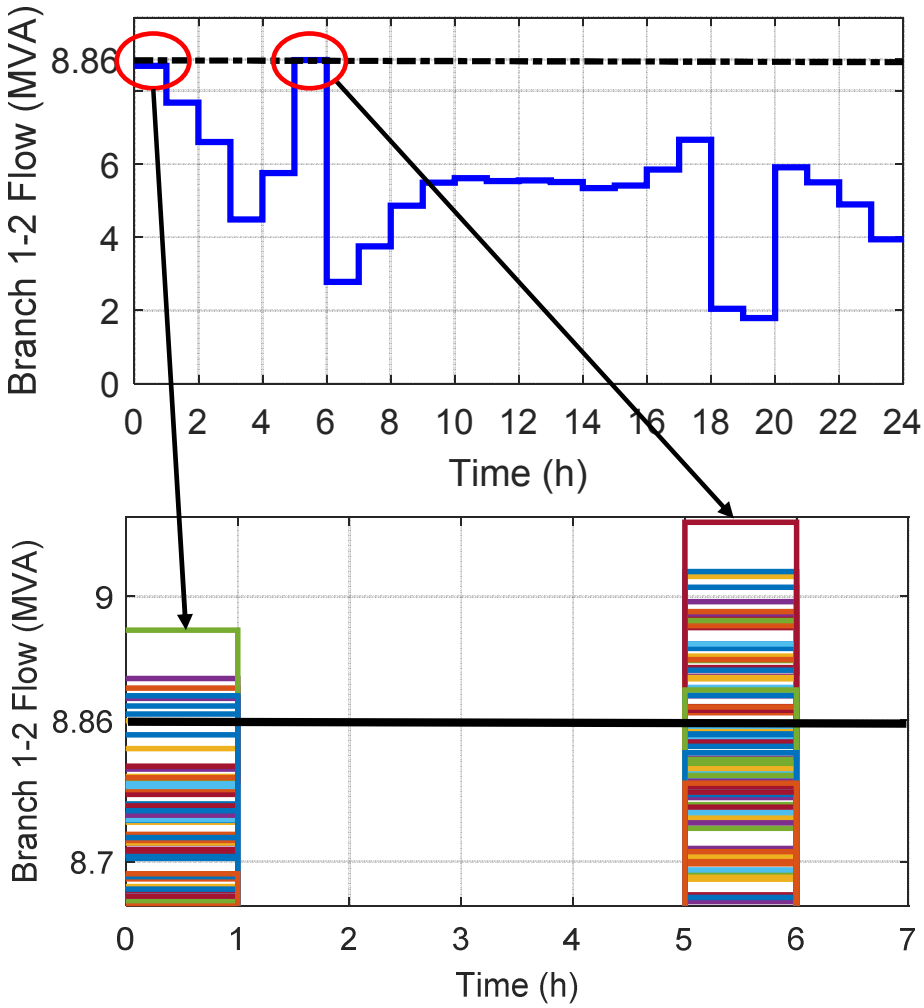

Figure 30: Impact of 10% demand (including EVs) uncertainty; feeder demand exceeds thermal limit with a probability of 45.31%. Lines in different colours represent different possible outcomes for feeder demand at midnight and at 05:00.

Table XIII: PoV for various values of w_L

w_L	PoV
1.0	45.31%
1.1	10.67%
1.2	3.21%
1.3	0.1%
1.35	0%

As the value of w_L increases, demand peak is lowered (see Figure 27) because EV charging is better distributed over time during the night (see Figure 26 at 00:00 – 06:00). This provides additional headroom and thus reduces the risk of violating the thermal limit. We have used the term PoV to express this here.

Consequently, incorporating loss cost (with an adjustable weight w_L) in aggregator's objective function can not only increase the EV hosting capacity of the feeder, but also manage the risk of violating line thermal limits.

Finally, we illustrate in Figure 31 the resulting feeder demand (100 possible outcomes) for w_L = 1.35 which presents a lower peak and explains the zero PoV obtained for this value.

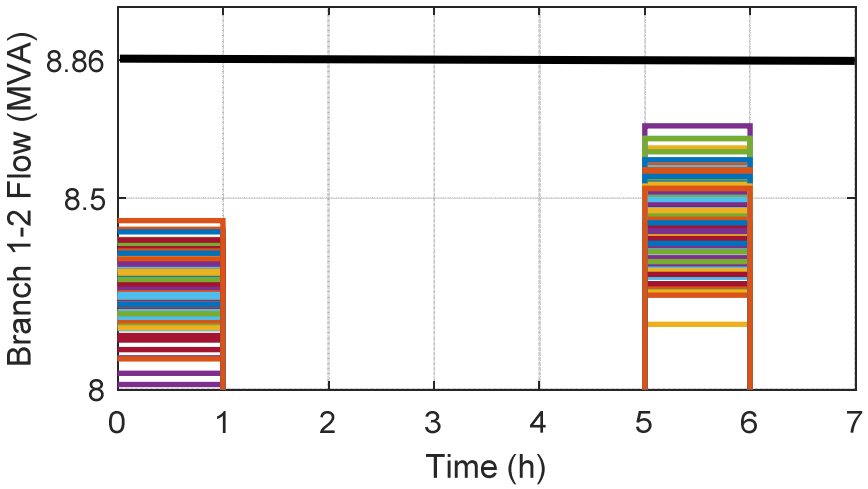

Figure 31: 100 possible outcomes of feeder demand with 10% uncertainty (normal distribution – including EVs) and w_L = 1.35. Feeder demand does not exceed thermal limit; PoV = 0%. Lines in different colours represent different possible outcomes for feeder demand.

5.3. Key Learning Points

- EVs have the potential to significantly affect network losses, in addition to voltage profiles, thermal limits etc.
- Single party decision making in a DNO/DSO world could lead to inefficient network utilization when considering EV actions (charging / discharging).
- DNO/DSO signaling of losses into aggregator decision-making can increase the EV hosting capacity in a distribution network and reduce costs for customers.

6. Conclusions

Firstly, this report has presented a novel loss estimation method, including feeder clustering. Initial results have proven to be promising in terms of providing a generic loss estimation tool, although additional further work is required to determine its usefulness in assessing losses across a larger set of test networks, and ultimately across all DNO/DSO controlled networks.

In addition to presenting a novel loss estimation method, this report has delivered enhanced understanding regarding network losses in three distinct areas, network reconfiguration, the introduction of SOPs, and in terms of EV actions within a given network area.

Firstly, in terms of network reconfiguration, it has been shown for a representative network case, that by optimising network configuration for loss minimisation, around a 40% reduction can be made against the original base case. This result should, however, be taken in context. A key factor when interpreting this result, is that it presents an upper limit, where the DNO/DSO has set loss reduction as its primary target. Clearly DNO/DSOs have other roles to play, not least in assisting to deliver the overall low carbon agenda, a factor which could indeed lead to an overall increase in network losses. This result merely indicates that if DNO/DSOs were sufficiently incentivised to include network losses in their active decision making, they have the potential to make significant effects to overall system loss minimisation. It should also be noted that whilst loss reduction is in this scenario the primary objective; it is not the only network parameter which can be affected. An additional benefit was an observed improvement in feeder voltage profile. Whilst there is an overall decrease in voltage drop, the most significant result of this profile improvement is in a tightening of the overall voltage bandwidth, allowing for greater control of upstream busbars and increased potential in terms of overall Active Network Management solutions, a factor which could play a significant role in delivering the low carbon transition. It was also demonstrated that there is strong synergy between reducing losses and improving reliability, and that a network optimised for low losses will be close to the same network optimised for reliability, and vice versa.

The findings around network reconfiguration were complemented by the introduction of Soft Open Points (SOPs). Using an SOP to interconnect two feeders has been shown to also have a significant effect on loss reduction, offering slightly more improvement than reconfiguration if the SOP is adequately sized and has high efficiency. Improvements in loss reduction using SOPs has an upper limit, at which point load balance is achieved between the two feeders. Beyond this point, increasing the rating of the SOP will have no effect in terms of loss reduction, and as such it can be determined that the greater the imbalance between the two feeders, the more an SOP can contribute towards loss reduction. Whilst it is potentially unlikely that an SOP is installed purely for reasons of loss reduction, such a device can provide additional benefits to business activities, such as providing flexible interconnection

between network areas, enhancing security of supply, or providing novel connection arrangements for increased embedded generation.

Finally, an example of decision-making incorporating losses within a future DSO scenario has been explored based on EV charging and discharging actions. . Here an external aggregator is theorised to optimally control its fleet in terms of profit seeking and makes these actions independent of cost-reflective losses charging within a DSO controlled network area. In this case, due to these independent, market driven actions there is the potential to significantly affect feeder loading, network thermal limits, voltage profiles, and network losses.

This would mean that in this effectively 'aggregator only' decision-making scenario, in order to maintain safe overall network operation, the aggregator would need to receive some form of signal from the DSO to simply reduce the number of controllable vehicles in its fleet, thus reducing thermal limit or voltage violations, but resulting in a net decrease in carbon reduction. The results in this report have shown however that if DNO/DSOs were to incorporate a losses charge for active network users (with an adjustable weight w_L) this can increase the EV hosting capacity in a distribution network. This case study showed an increase of 45% (803 EVs → 1,165 EVs). Adjusting the weight w_L allows for management of the thermal limit violation risk. In our example demonstration case, a weight value of $w_L = 1$ results in a probability of violation (PoV) of 45.31%, whilst increasing the weight value to $w_L = 1.35$ decreases the PoV value to 0%.

As a result of these findings, it could be extrapolated that single party decision making in a DNO/DSO world will lead to inefficient network utilization when considering EV actions (charging / discharging). This case study again reinforces the fact that whilst loss reduction remains a primary objective, additional network parameters are affected and often improved. One aspect of Northern Powergrid's Customer-Led Distribution System (CLDS) project aims to explore links between the actions of system stakeholders, independent, uncertain or otherwise, and the necessary actions of the DSO to preserve system integrity. Defining the required shape, scale, location and magnitude etc. of these DSO procured flexibility contracts and the degree to which the actions of others can deliver similar benefits is a key aspect of the research being undertaken. This project has shown that signaling available network capacity in the form of active losses charging offers a potential mechanism by which the DSO could increase overall system efficiency and maintain integrity within the distribution system. Each

of these three areas of investigation has shown that a DNO/DSO has significant potential to affect their networks in terms of reducing network losses. Clearly an effective charging incentive will be required to motivate DNOs in terms of adopting these measures, however the results shown in this report have highlighted that if losses are not taken into account in future likely DSO scenarios, there is a high likelihood that this will result in inefficient and high cost utilization of distribution networks.

7. References

[1] A. K. Dashtaki and M. R. Haghifam, "A New Loss Estimation Method in Limited Data Electric Distribution Networks," *IEEE Trans. Power Del.*, vol. 28, no. 4, pp. 2194-2200, 2013, doi: 10.1109/TPWRD.2013.2273103.

[2] Element Energy. *Element Energy Load Growth (EELG) Datasets*.

[3] R. J. Broderick and J. R. Williams, "Clustering methodology for classifying distribution feeders," in *2013 IEEE 39th Photovoltaic Specialists Conference (PVSC)*, 16-21 June 2013 2013, pp. 1706-1710, doi: 10.1109/PVSC.2013.6744473.

[4] V. Rigoni, L. F. Ochoa, G. Chicco, A. Navarro-Espinosa, and T. Gozel, "Representative Residential LV Feeders: A Case Study for the North West of England," *IEEE Trans. Power Syst.*, vol. 31, no. 1, pp. 348-360, 2016, doi: 10.1109/TPWRS.2015.2403252.

[5] MathWorks. "k-means clustering." https://uk.mathworks.com/help/stats/kmeans.html.

[6] MathWorks. "Silhouette criterion clustering evaluation object." https://uk.mathworks.com/help/stats/clustering.evaluation.silhouetteevaluation-class.html.

[7] MathWorks. "Construct agglomerative clusters from linkages." https://uk.mathworks.com/help/stats/cluster.html.

[8] I. Sarantakos, D. M. Greenwood, J. Yi, S. R. Blake, and P. C. Taylor, "A method to include component condition and substation reliability into distribution system reconfiguration," *Int. J. Elect. Power Energy Syst.*, vol. 109, pp. 122-138, 2019, doi: https://doi.org/10.1016/j.ijepes.2019.01.040.

[9] J. Zhu, *Optimization of Power System Operation*, 2nd ed. New Jersey: Wiley-IEEE Press, 2015.

[10] Centre for Sustainable Electricity and Distributed Generation at Imperial College London. "United Kingdom Generic Distribution System." https://github.com/sedg/ukgds.

[11] W. Kocay and D. Kreher, *Graphs, Algorithms, and Optimization* (Discrete Mathematics and Its Applications). CRC Press, 2004.

[12] Z. Ghofrani-Jahromi, M. Kazemi, and M. Ehsan, "Distribution Switches Upgrade for Loss Reduction and Reliability Improvement," *IEEE Trans. Power Del.*, vol. 30, no. 2, pp. 684-692, Apr. 2015, doi: 10.1109/TPWRD.2014.2334645.

[13] A. M. Tahboub, V. R. Pandi, and H. H. Zeineldin, "Distribution System Reconfiguration for Annual Energy Loss Reduction Considering Variable Distributed Generation Profiles," *IEEE Trans. Power Del.*, vol. 30, no. 4, pp. 1677-1685, Aug. 2015, doi: 10.1109/TPWRD.2015.2424916.

[14] A. Asrari, S. Lotfifard, and M. Ansari, "Reconfiguration of Smart Distribution Systems With Time Varying Loads Using Parallel Computing," *IEEE Trans. Smart Grid*, vol. 7, no. 6, pp. 2713-2723, Nov. 2016, doi: 10.1109/TSG.2016.2530713.

[15] R. N. Allan, R. Billinton, I. Sjarief, L. Goel, and K. S. So, "A reliability test system for educational purposes – Basic distribution system data and results," *IEEE Trans. Power Syst.*, vol. 6, no. 2, pp. 813-820, May 1991, doi: 10.1109/59.76730.
[16] "Information from Northern Powergrid DNO, UK," 2020.
[17] MathWorks. "Find Pareto front of multiple fitness functions using genetic algorithm." https://uk.mathworks.com/help/gads/gamultiobj.html.
[18] Elexon. "Load Profiles." https://www.elexon.co.uk/operations-settlement/profiling/.
[19] W. Cao, J. Wu, N. Jenkins, C. Wang, and T. Green, "Benefits analysis of Soft Open Points for electrical distribution network operation," *Appl. Energy*, vol. 165, pp. 36-47, Mar. 2016, doi: https://doi.org/10.1016/j.apenergy.2015.12.022.
[20] E. Romero-Ramos, A. Gómez-Expósito, A. Marano-Marcolini, J. M. Maza-Ortega, and J. l. Martinez-Ramos, "Assessing the loadability of active distribution networks in the presence of DC controllable links," *IET Gener. Transm. Distrib.*, vol. 5, no. 11, pp. 1105-1113, 2011, doi: 10.1049/iet-gtd.2011.0080.
[21] P. Li *et al.*, "Coordinated Control Method of Voltage and Reactive Power for Active Distribution Networks Based on Soft Open Point," *IEEE Trans. Sustain. Energy*, vol. 8, no. 4, pp. 1430-1442, 2017, doi: 10.1109/TSTE.2017.2686009.
[22] C. Wang, G. Song, P. Li, H. Ji, J. Zhao, and J. Wu, "Optimal Configuration of Soft Open Point for Active Distribution Network Based on Mixed-integer Second-order Cone Programming," *Energy Procedia*, vol. 103, pp. 70-75, 2016/12/01/ 2016, doi: https://doi.org/10.1016/j.egypro.2016.11.251.
[23] A. Aithal, G. Li, J. Wu, and J. Yu, "Performance of an electrical distribution network with Soft Open Point during a grid side AC fault," *Appl. Energy*, vol. 227, pp. 262-272, 2018, doi: https://doi.org/10.1016/j.apenergy.2017.08.152.
[24] Gurobi Optimization LLC. "Gurobi Optimizer Reference Manual." http://www.gurobi.com.
[25] MOSEK ApS. "The MOSEK Optimization Tools Version 9.0." http://www.mosek.com/.
[26] IBM. "IBM ILOG CPLEX Optimization Studio." www.cplex.com.
[27] Elexon. "Price Profiles." https://www.bmreports.com/bmrs/?q=balancing/marketindex

8. Appendix

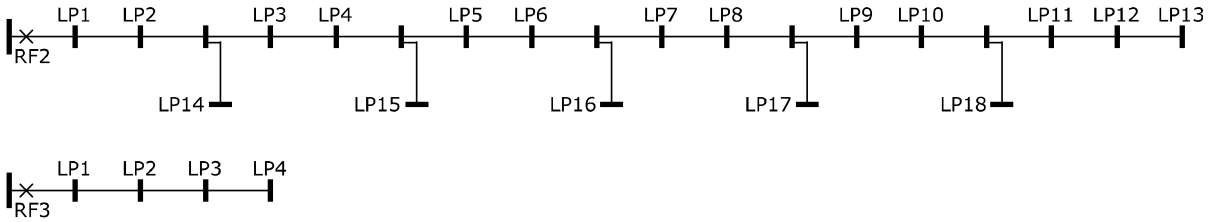

Figure 32: Representative feeders of Clusters 2 and 3.

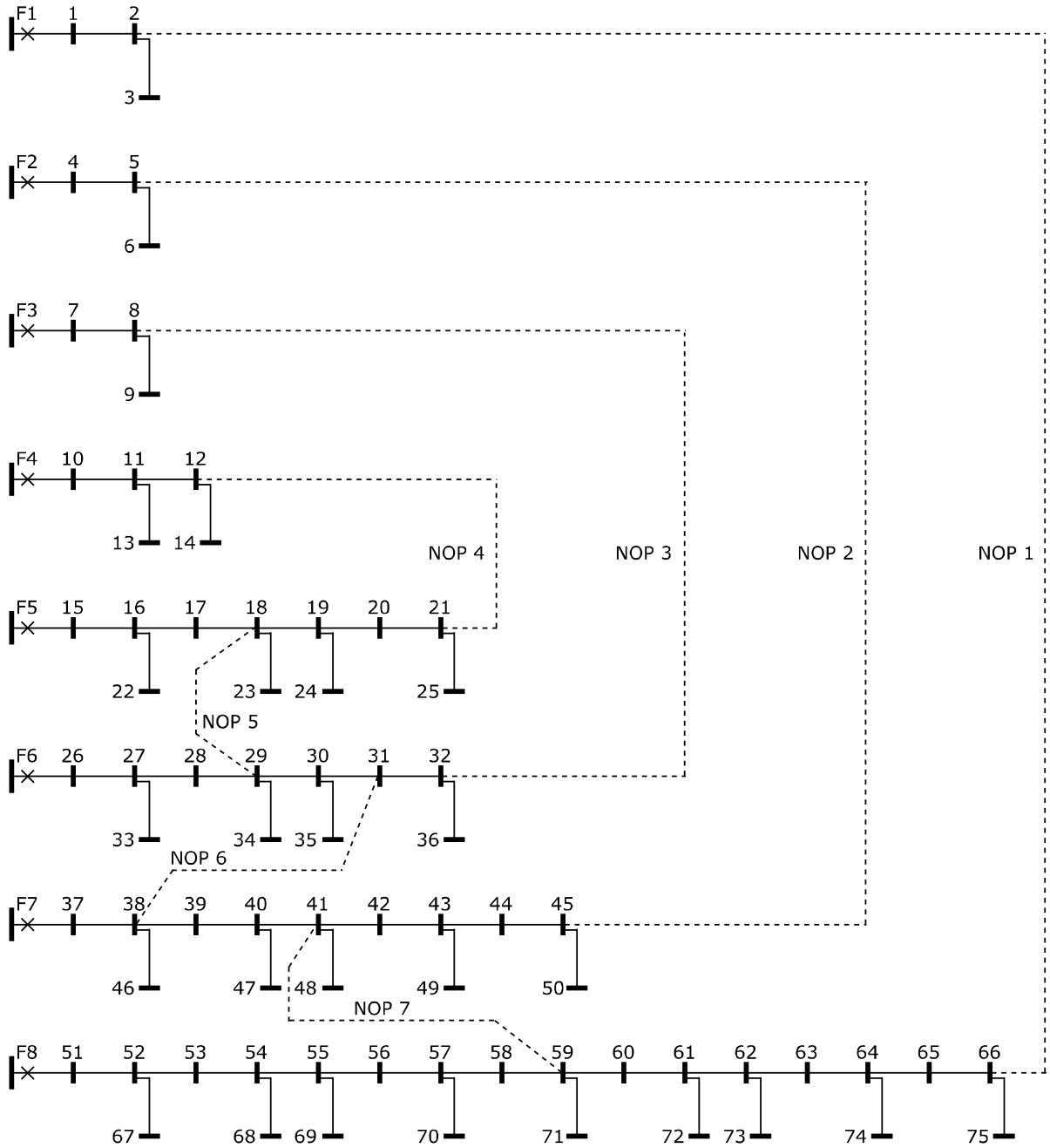

Figure 33: HV UG UKGDS with seven normally open points.

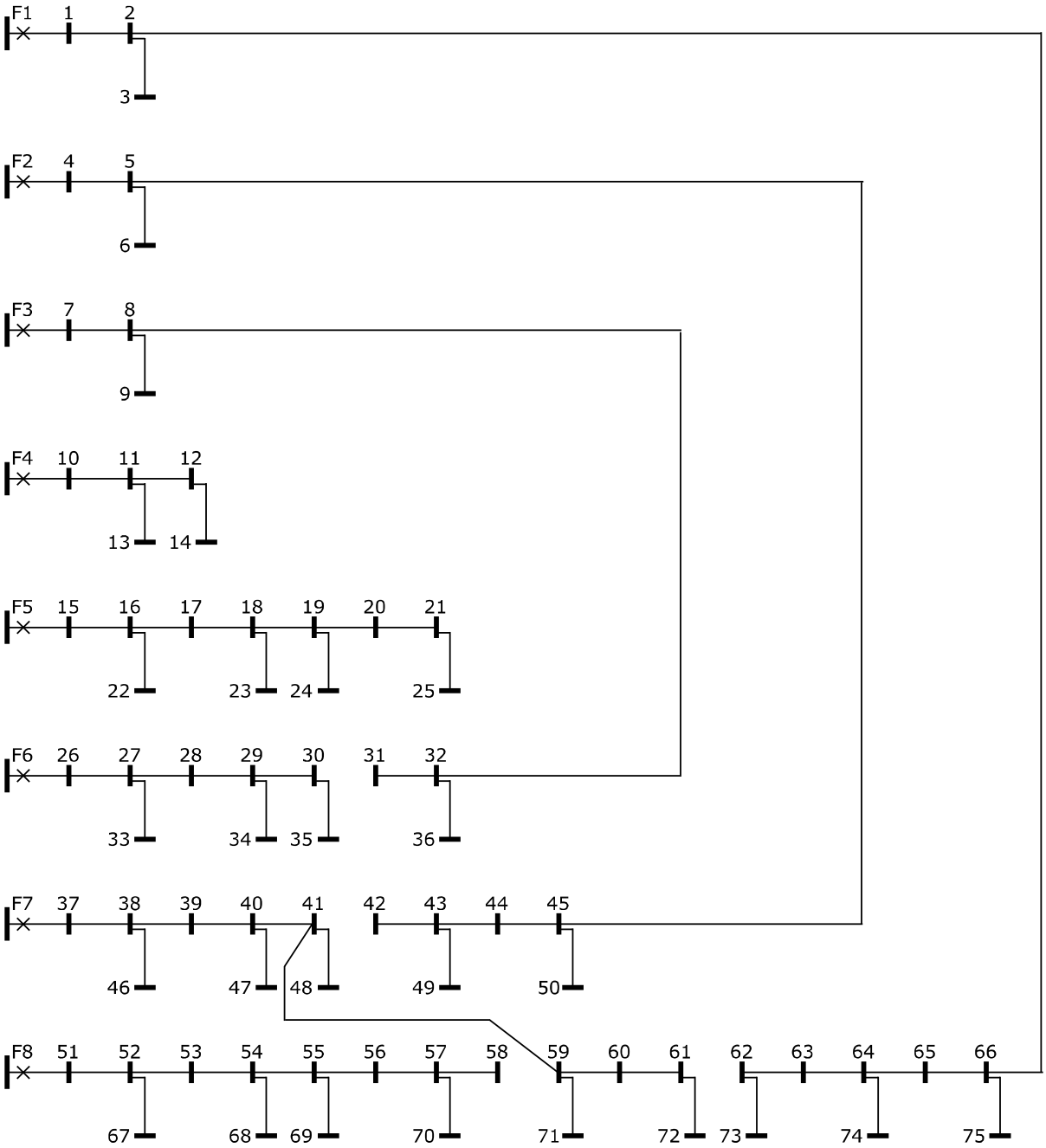

Figure 34: Optimal network configuration for Section 3.3.

Table XIV: Customer types for the HV UG UKGDS.

Customer Type	Elexon Profile Class	Load Points (Buses)
Residential	1	1, 3-6, 10, 12, 14, 17-19, 21, 23, 25-27, 32-38, 40, 42, 44-47, 50, 52, 54, 57-59, 61, 63-65, 68-69, 71, 73-75
Commercial	3	2, 7-9, 11, 13, 15-16, 20, 22, 24, 28-31, 39, 41, 43, 48-49, 51, 53, 55-56, 60, 62, 66-67, 70, 72